ซีโอไลต์รูพรุนเมโซชนิด NaY สำหรับการดูดซับก๊าซไฮโดรเจนคลอไรด์

นางสาว ธาราภรณ์ ยางเยี่ยม

วิทยานิพนธ์นี้เป็นส่วนหนึ่งของการศึกษาตามหลักสูตรปริญญาวิทยาศาสตรมหาบัณฑิต
สาขาวิชาการจัดการสิ่งแวดล้อม (สหสาขาวิชา)
บัณฑิตวิทยาลัย จุฬาลงกรณ์มหาวิทยาลัย
ปีการศึกษา 2553

MESOPOROUS ZEOLITE NaY FOR HYDROGEN CHLORIDE ADSORPTION

Miss Tharaporn Yangyaim

A Thesis Submitted in Partial Fulfillment of the Requirements

for the Degree of Master of Science Program in Environmental Management

(Interdisciplinary Program)

Graduate School

Chulalongkorn University

Academic Year 2010

Thesis Title   MESOPOROUS ZEOLITE NaY FOR HYDROGEN
                      CHLORIDE ADSORPTION

By   Miss Tharaporn Yangyaim

Field of Study   Environmental Management

Thesis Advisor   Associate Professor Nurak Grisdanurak, Ph.D.

Accepted by the Graduate School, Chulalongkorn University in Partial Fulfillment of the Requirements for the Master's Degree

.... Dean of the Graduate School

(Associate Professor Pornpote Piumsomboon, Ph.D.)

THESIS COMMITTEE

....Chairman

(Assistant Professor Chantra Tongcompou, Ph.D.)

....Thesis Advisor

(Associate Professor Nurak Grisdanurak, Ph.D.)

....Examiner

(Associate Professor Jin Anotai, Ph.D.)

....Examiner

(Patiparn Punyapalakul, Ph.D.)

....External Examiner

(Pongtanawat Khemthong, Ph.D.)

ธาราภรณ์ ยางเยี่ยม : ซีโอไลต์รูพรุนเมโซชนิด NaY สำหรับการดูดซับก๊าซไฮโดรเจนคลอ
ไรด์ (MESOPOROUS ZEOLITE NaY FOR HYDROGEN CHLORIDE ADSORPTION)
อ. ที่ปรึกษาวิทยานิพนธ์หลัก : รศ.ดร. นุรักษ์ กฤษดานุรักษ์, 82 หน้า.

สารประกอบไฮโดรเจนคลอไรด์ (HCl) ในปริมาณน้อยซึ่งปนเปื้อนอยู่ในก๊าซไฮโดรเจน
อาจส่งผลกระทบต่อกระบวนการปลายทางที่ใช้ก๊าซไฮโดรเจนเป็นสารป้อน ดังนั้นการศึกษานี้จึง
มุ่งเน้นการกำจัด HCl ด้วยตัวดูดซับเมโซพอรัสซีโอไลต์วาย (Meso-NaY) การเตรียมเมโซพอรัสซี
โอไลต์ทำได้ในสองรูปแบบคือ Meso-NaY (Leaching) และ Meso-NaY (Template) จะถูก
ทำการศึกษาการดูดซับและวิเคราะห์คุณลักษณะด้วยเทคนิคการเลี้ยวเบนของรังสีเอกซ์ การดูด
ซับ-คายซับของก๊าซไนโตรเจน กล้องจุลทรรศน์อิเล็กตรอนแบบส่องกราด เอกซเรย์ฟลูออเรสเซนส์
และฟูเรียร์ทรานส์ฟอร์มอินฟาเรด พบว่า มีโครงสร้างผลึกเอกลักษณ์ ขนาดผลึก แบบเดียวกับซี
โอไลต์วายแต่มีค่าพื้นที่ผิว และปริมาตรรูพรุน เพิ่มขึ้น โดยให้ประสิทธิภาพการดูดซับ HCl สูงกว่า
สารดูดซับทางการค้า โดยผลการเติมประจุบวกของแมกนีเซียม ลงบน Meso-NaY (Leaching) จะ
ทำให้พื้นที่ผิวมีค่าลดลงมากกว่า 50% และไม่มีส่วนเพิ่มประสิทธิภาพการดูดซับ HCl สำหรับการ
ขึ้นรูป Meso-NaY (Leaching) ที่ศึกษาทั้ง 3 วิธี คือ การอัดแรงดัน การเคลือบเชิงกล และการอัด
ฉีด พบว่า Meso-NaY (Leaching) จากวิธีด้วยการอัดแรงดันสามารถใช้ซ้ำและยืนยัน
ประสิทธิภาพการดูดซับ ซึ่ง Meso-NaY (Leaching) ให้ค่าการดูดซับ เท่ากับ 0.1985 กรัมของ HCl
ต่อกรัม นอกจากนี้ตัวดูดซับที่ใช้แล้วจะเกิดผลึกของเกลือในโครงสร้าง

สาขาวิชา <u>การจัดการสิ่งแวดล้อม</u>   ลายมือชื่อนิสิต......ธาราภรณ์   ยางเยี่ยม.....................
ปีการศึกษา 2553   ลายมือชื่อ อ.ที่ปรึกษาวิทยานิพนธ์หลัก....................

5287536020 : MAJOR ENVIRONMENTAL MANAGEMENT

KEYWORDS : RICE HUSK SILICA / HYDROGEN CHLORIDE / MESO-NaY

THARAPORN YANGYAIM : MESOPOROUS ZEOLITE NaY FOR HYDROGEN CHLORIDE ADSORPTION. ADVISOR : ASSOC. PROF. NURAK GRISDANURAK, Ph.D., 82 pp.

Trace amount of hydrogen chloride (HCl) contaminated in hydrogen (H_2) feed stock which affects to downstream chemical processes. Thus, the removal of HCl gas over Meso-NaY was a focus. Meso-NaY by two synthesis methods (leaching and template) were studied. Material was characterized by X-ray Diffraction (XRD), N_2 adsorption-desorption, Scanning Electron Microscopy (SEM), X-ray Fluorescence (XRF) and Fourier Transform Infrared (FTIR). The phase and crystallite size of Meso-NaY showed the same structure as zeolite NaY. However, the surface area and the pore volume of Meso-NaY were increased, resulting higher HCl adsorption capacity compared to a commercial adsorbent. The effect of Mg positive charge adding into Meso-NaY lowered surface area by 50% and provided lower HCl removal than itself. Three methods of pelletization of Meso-NaY (Leaching) including pressing, mechanical coating, and extrusion, were studied. The pellet obtained by pressing metod provided higher surface area and adsorption performance of HCl with adsorption potential (W_b) of 0.1985 $g_{HCl}/g_{adsorbent}$. Moreover, spent adsorbent maintained sodium chloride in its structure.

ศูนย์วิทยทรัพยากร
จุฬาลงกรณ์มหาวิทยาลัย

Field of Study: Environmental Management Student's Signature. THARAPORN YANGYAIM

Academic Year: 2010 Advisor's Signature. $2u$ นฟ

ACKNOWLEDGEMENTS

CONTENTS

LIST OF TABLES

LIST OF FIGURES

LIST OF ABBREVIATIONS

ºC	Degree celsius
μ	Micron
λ	Lambda
Ɵ	Theta
Al	Aluminum
AlO_4	Aluminum
Al_2O_3	Aluminium(III) oxide
Ca^{2+}	Calcium ion
cm	Centimeter
CTAB	Hexadecyltrimethylammonium bromide
Cu	Copper
CuCl	Copper (I) chloride
$CuSO_4$	Copper sulfate
$Cu(OH)_2$	Copper hydroxide
g	Gram
h	Hour
H^+	Hydrogen ion
H_2	Hydrogen gas
HCl	Hydrochloric acid
L	Liter
Kg	Kilogram
mA	Miliampere
mg	Milligram
Mg^{2+}	Magnesium ion
min	Minute
mL	Mililitter
Mg	Mangasium
$Mg(NO_3)_2 \cdot 6H_2O$	Magnesium nitrate hexahydrate
MgO	Magnesium oxide
N_2	Nitrogen
Na^+	Sodium ion

$NaAlO_2$	Sodium aluminate
$NaCl$	Sodium chloride
Na_2O	Sodium oxide
$NaOH$	Sodium hydroxide
Na_2SiO_3	Sodium silicate
P	Total pressure
P_0	Saturation vapor pressure
PDADMAC	Poly diallydimethylammonium chloride
ppm	Part per million
SiO_2	Silicon dioxide
V	Volt
W	Watt
$ZnCl_2$	Zinc chloride
ZnO	Zinc oxide

CHAPTER I

INTRODUCTION

1.1 Introduction

The trace amount of chlorine and chlorinated hydrocarbon compounds in downstream chemical processes can be converted to hydrogen chloride (HCl) during the flow. HCl is a toxic gas. It can corrode pipe-line and poison catalyst (Hue et al., 1986). It has been reported by Twigg and Spencer (2001) that reactivity of $Cu/ZnO/Al_2O_3$ on water gas shift reaction was reduced from 100 to 60% when feedstock was contaminated by HCl only 0.03% in input feed. Therefore, it has been a strong force to remove HCl gas by adsorption method. There are many types of adsorbents used for HCl removal such as activated carbon and metal oxides (KO, CaO, MgO) (Hue et al., 1986; Park and Jin, 2005). However, activated carbon and metal oxides give low adsorption efficiency due to having no active metal and possessing low surface area, respectively. Zeolite NaY is an alternative material for considering as an effective adsorbent. It is a micropore crystalline aluminosilicate which consists of SiO_4 and AlO_4 in the faujasite family. It has high surface area and contains with sodium content (Yang, 2003; Wittayakun and Grisdanurak, 2004). In our laboratory, commercial adsorbent has been studied on HCl adsorption against synthesized zeolite NaY. It was reported that synthesized zeolite NaY showed the potential of HCl adsorption equally to the commercial one. The development of zeolite NaY is interested in this study.

This study focuses on the use of rice husk as an alternative source of silica for the synthesis. It is not only having a main composition of silica more than 90% but also this is the way for increasing valuable of waste (Rahman et al., 2009). To enhance the adsorption efficiency, the zeolite NaY must posse's mesopore material with positive charge in extra-framework. The Meso-NaY can be synthesized in various ways such as a chemical treatment method by leaching zeolite NaY with NaOH for creating mesopores (Abello et al., 2009). Another technique is using template to generate mesopores, however, less positive charge was generated than the chemical treatment method (Liu et al., 2008). Afterward, Meso-NaY should be

modified by adding positive charge of metal on surface to increase for HCl-adsorbed sites (McWilliams et al., 1988; Lee et al., 2003; Hue et al., 1986). The Ag and Ni nanoparticles had been used as active metal for HCl removal (Kim et al., 2008, Park and Jin, 2005). However, electroplating method and transition metals are high cost and not be applicable to gaseous removal. The guard adsorbent which consists of alkaline earth metal oxide such as calcium (Ca) and magnesium (Mg) on ZSM5-zeolite had been used for removing trace amount of organic chlorides form feed stock. Nevertheless, the electronegativity value of Mg is of high (1.31) among other alkaline earth elements. It is expected that the high attraction force of an atom for shared electrons and effective than calcium (Chang et al., 2007; Hua et al., 1976; McWilliams et al., 1988). Therefore, the addition of magnesium oxide (MgO) is performed in this study for increasing of active site in structure of zeolite NaY. The form of adsorbent which used in HCl adsorption should be considered since the shape of adsorbent might be effect the adsorption efficiency. The adsorbent in powder form can cause high pressure drop during the use. The pellet form could be suggested. There are several methods for pelletization such as pressing under pressurized, mechanical coating, and extrusion. All of these pelletizations would be applied (McWilliams et al., 1988; Rahman et al., 1994; Yoshida et al., 2009). In this study, all adsorbents are investigated for removing HCl in a continuous fixed-bed reactor.

1.1 Objectives

1. To synthesize mesoporous zeolite NaY with magnesium (Mg/Meso-NaY) from rice husk silica.
2. To evaluate the synthesized material on the removal of hydrogen chloride (HCl) contaminated in natural gas under a flow system.

1.2 Hypothesis

Mg/Meso-NaY is able to adsorb HCl comparing to general adsorbent.

1.3 Scopes of the study

1. Meso-NaY is synthesized from rice husk.
2. Magnesium is used as a cation to modify the obtained material (Mg/Meso-NaY).
3. All three methods of pelletization are used to prepare the granular adsorbents.
4. Hydrogen chloride concentration used in this study is 500 ppm.

CHAPTER II

BACKGROUND AND LITERATURE REVIEWS

2.1 Hydrogen chloride

Chlorinated hydrocarbons or chlorine contaminated in small amount in hydrogen feed stock for industrial process can be converted to HCl. HCl is a colorless, nonflammable gas with an acid odor as shown in Table 2.1 (Lewis and Whitman, 1924). Gaseous HCl is poison chemical for downstream catalyst, generating hazardous solid waste. When it is mixed with moisture or water, hydrochloric acid solution or mist could be formed known as hazardous substance.

Table 2.1 HCl properties (Lewis and Whitman, 1924)

Properties	Identification
IUPAC name	Hydrogen chloride
Molecular formula	HCl
Molar mass	36.46 g/mol
Appearance	Colorless gas
Density	1.477 g/L, gas (25°C)
Melting point	-114.2°C
Boiling point	85.1°C
Solubility in water	72 g/100 mL (20°C)
Solubility equation in water	$HCl\ (aq) \longrightarrow H^+(aq) + Cl^-(aq)$
Hazards	Poison, corrosive In form of liquid and mist cause severe burns to all body tissue and may be fetal when swallowed or inhaled; lung damage
IDLH (ppm)	50

The high concentration of HCl can affect the health because of its corrosiveness. It also corrodes pipeline of downstream processes and poisons catalyst in downstream reactions such as water-gas-shift reaction with the slight increase in the amount of chloride in feed gas, it highly affects its performance as shown in Figure 2.1 (Hue et al., 1976; McWilliams et al., 1988; Sechrist et al., 1988; Twigg and Spencer, 2001). Therefore, it has been of interest to remove HCl by adsorption.
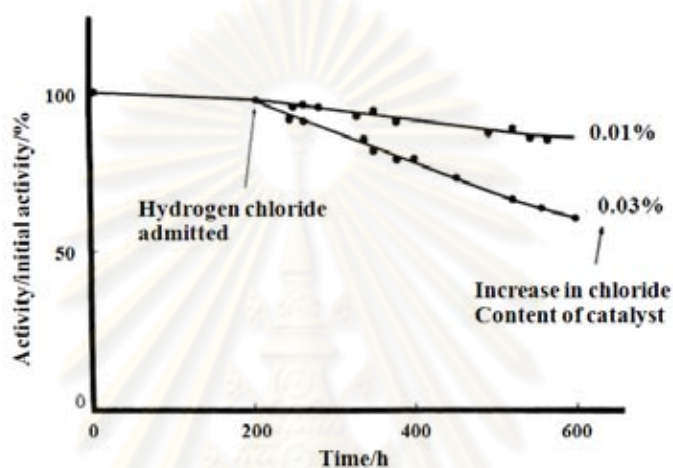
Figure 2.1 Deactivity of water-gas-shift caused by raising amount of HCl in the feed gas on $Cu/ZnO/Al_2O_3$ (Twigg and Spencer, 2001).

Figure 2.1 is an example to explain the declination of water-gas-shift catalyst $(Cu/ZnO/Al_2O_3)$ activity affecting by different concentrations of HCl. Therefore, HCl in hydrogen feed stock is required to be reduced in order to damage or generate more hazardous wastes. The removal of chloride contaminated in hydrogen feed stock consists of two systems, including hydrotreatment unit and chloride guard beds shown in Figure 2.2. The flow of chlorine compound passes through the column which contains catalyst. In the reactor, hydrogen gas is converted to HCl. Then, HCl is flowed through Cu or ZnO acting as chloride guards that readily to adsorb on Cu or ZnO as shown in equation 2-1 to 2-2.

$$Cu(s) + 2HCl(g) \longrightarrow CuCl + \frac{1}{2} H_2O(g) \qquad (2\text{-}1)$$

$$ZnO(s) + 2HCl(g) \longrightarrow ZnCl_2 + H_2O(g) \qquad (2\text{-}2)$$
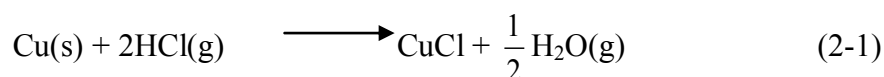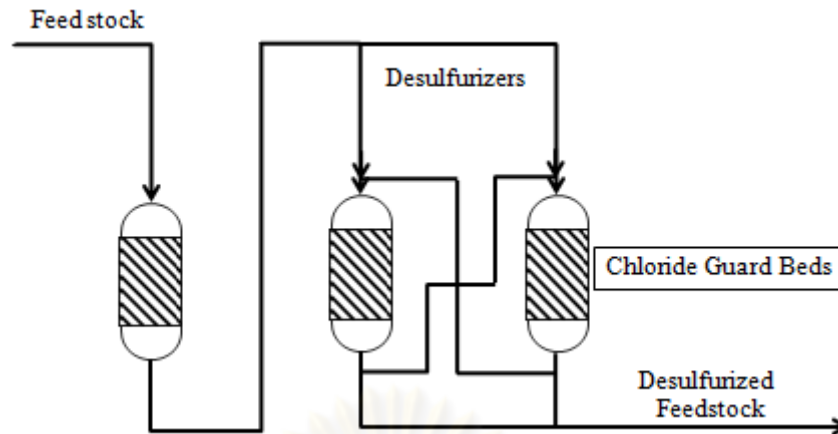
Figure 2.2 Chloride guard process (Twigg and Spencer, 2001).

2.2 Adsorption

Adsorption occurs when the adsorbates in the form of gas or liquid accumulate onto a surface of adsorbent. Generally, the adsorption is classified as exhibiting physisorption or chemisorption. The physisorption is the reaction of interacting between dipole and dipole molecules resulting in the weakly force of intermolecular by Van der Waals and/or force of dispersion. The chemisorption is the reaction between adsorbate molecule and the surface of adsorbent molecule in the strongly force. The adsorptive separation can perform efficiently that depends on quality of adsorbent (Crittenden and Thomas, 1998; Keller and Sraudt, 2005; Grisdanurak et al., 2004; Ruthven, 1984).

The most important factors affecting gas adsorption include
- Surface area of adsorbent
- Particle size of adsorbent: particle in small size reduces internal diffusion and mass transfer limitation in term of the penetration of the adsorbate inside the adsorbent
- Flow rate: low flow rate of adsorbate in gas phase passing through the adsorbent increases adsorption contact time
- Moisture content or humidity: moisture more than 50% reduces the efficiency of adsorption.

The main factor of HCl removal is amount of cation metals appeared in the absorbent structure, while the minor factor of HCl removal is the pore size and the surface area. There are many types of adsorbents which have been used for HCl removal such as activated carbon with nickel and metal oxides (KO, CaO, MgO) (Hua et al., 1976; Park and Jin, 2005). However, activated carbon and metal oxides performed low adsorption efficiency because they had no active metal and low surface area, respectively. To overcome the problem of adsorption efficiency, the adsorbent must be composed of the both active metal and high surface area (Yang, 2003). Zeolite is one of material which contains both functions.

2.3 Zeolite NaY

Zeolite NaY has been used to adsorb ozone, chlorofluorocarbons (CFC) and carbon dioxide (CO_2) (Chatterjee et al., 2003; Walton et al., 2006). Zeolite NaY, faujasite zeolite is microporous crystalline aluminosilicates which consists of SiO_4 and AlO_4. The negative charge might be occurred when Si^{4+} is substituent by Al^{3+}. Afterward, the positive charge would be balanced to neutral composed of alkali or alkaline cation in an extra-framework in molar ratio $Na_{56}[Al_{56}Si_{136}O_{384}]\cdot250H_2O$ with Si/Al ratio of 2.43 and possess high surface area. It consists of linking of 6 sodalite units on its hexagonal faces as shown in Figure 2.3. The sodalite units might be formed from secondary and tertiary building blocks, which have SiO_4 and AlO_4 as primary building block. The structure of zeolite NaY consists of cavity or channel in diameter of 3-10 Å and supercage in diameter of 8 Å. The porous material is the characteristic of zeolite NaY providing of its potential selectivity in both adsorption and chemical reaction. Chemicals in smaller size than zeolite's cavity will be reacted over active sites.

Zeolite NaY can be synthesized by any source of silica. Rice husk has been studied extensively on silica source which is one way to reduce waste from rice milling (Chumee et at., 2009; Mohamed et al., 2008; Rahman et al., 1994; Rahman et al.2009; Walton et al., 2006; Wittayakun et al., 2007; Yang, 2003).
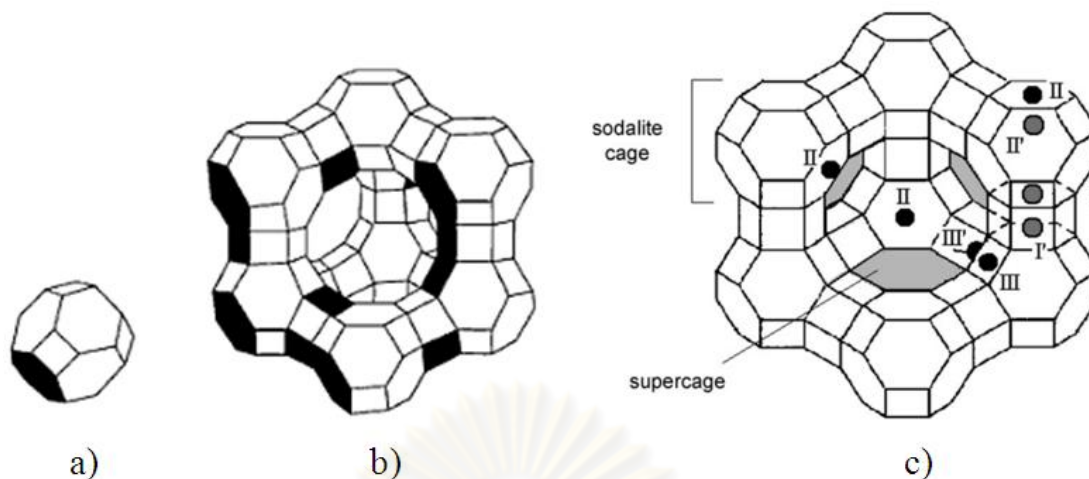
Figure 2.3 Zeolite NaY structure: a) sodalite cage, or beta cage or truncated octahedron; b) unit cell of zeolite NaY, or faujasite; c) cation site in type Y locate at site I, I', II and II' (Yang, 2003).

2.4 Rice husk silica

Rice husk is agricultural waste in Thailand which can utilize as fuel source in power plant. Moreover, it is widely use as silica source due to constituents of SiO_2 more than 90% in amorphous phase (Rahman et al., 2009). Silica is one of main constituents in zeolite NaY. Silica is not toxic and inert substance. There are two major types of silicas; natural and synthesized silica. Generally, natural silica is divided into classes:

1. Crystalline silica: This form depends on crystalline temperature. The structure would be formed in high crystallinity when temperature is increased. The main crystalline silica includes quartz, tridymite and cristobalite. The crystalline silica is showed in Figure 2.4 (a).

2. Amorphous silica; It has higher reactivity and porosity such as silica gel which prepared from sodium silicate. The amorphous silica structure is incompletely arrangement due to fast crystallization during the ageing as shown in Figure 2.4 (b).

a)   b)
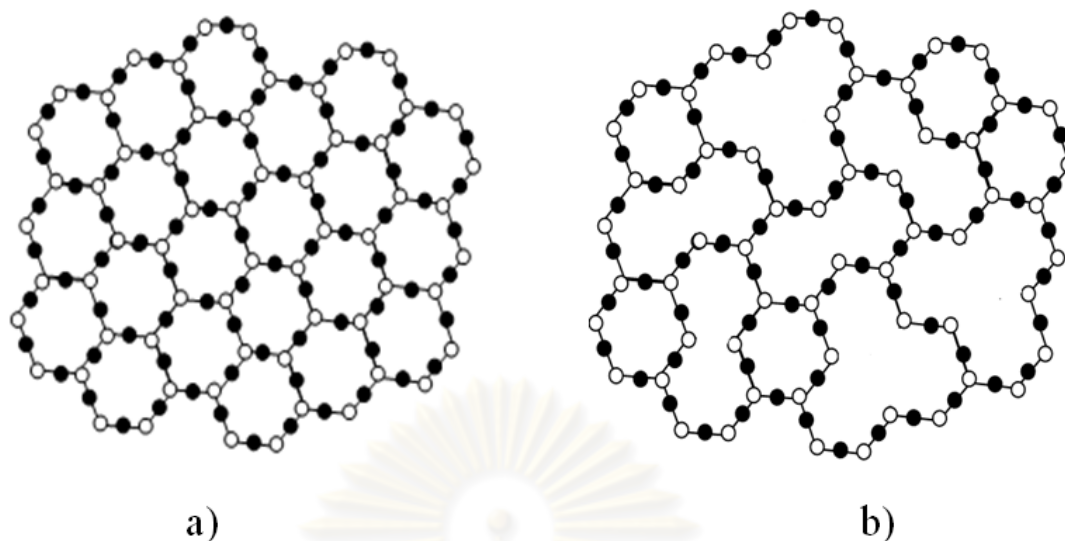
Figure 2.4 Silica: a) crystalline silica; b) amorphous silica
(Grisdanurak and Wittayakun, 2004).

2.5 Surface modification of zeolite

The modification of zeolite for having mesopores is one possible for enhancing the adsorption of larger kinetic-size chemical. Not only the pore enlargement, two modifications will be studies. They are positive charge impregnation and pelletization.

2.5.1 Pore enlargement

Two techniques are described have and be used to enlarge the micropore to mesopore. They are chemical treatments and adding template.

2.5.1.1 NaOH leaching

The chemical treatment is a leaching technique. It can be done by NaOH or hydrochloric acid. Figure 2.5 shows the slipping out of zeolite material texture under base condition. The texture of original Si/Al material was slipped out

higher than that of low Si/Al material (Abello et al., 2009; Realpe and Ramírez, 2010).
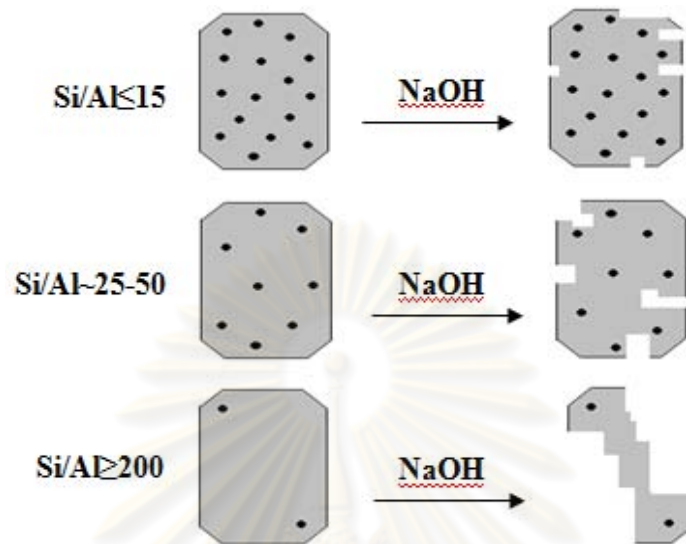
Figure 2.5 Formation of mesopores in different Si/Al ratios

(Realpe and Ramírez, 2010).

2.5.1.2 Forming through template

Another method is an addition of organic template such as hexadecyltrimethylammonium bromide (CTAB) and polydiallydimethylammonium chloride (PDADMAC). The template is added during the synthesis of zeolite NaY to create the mesopore into its structure. Accordingly, the template in form of micelle is catches with silica and alumina around the micelle and form to particle. The mesopore particle is obtained after calcinations (Garcı́a et al., 2005; Liu et al., 2008).
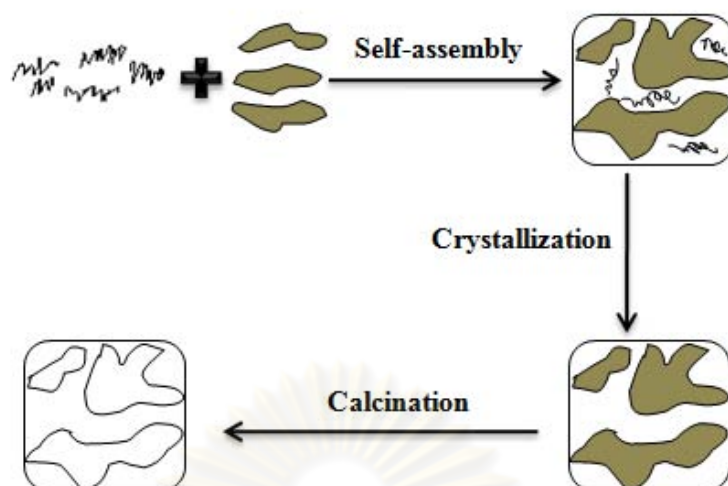
Figure 2.6 Schematic diagram of mesopore formation through cationic polymer template (Garcı′a et al., 2005).

2.5.2 Positive charges impregnation

The guard adsorbent is an important. It consists of alkaline earth metal oxide ZSM5-zeolite. Alkaline earth elements, such as calcium (Ca) and magnesium (Mg) have high electronegativity value. The electronegativity value of Mg is of high (1.31) among alkaline earth elements. It exhibits the attraction force of an atom for shared electrons and effective than calcium (Chang et al., 2007; Hua et al., 1976; McWilliams et al., 1988). Therefore, the addition of magnesium oxide (MgO) will be interested. Mg would increase active sites in the structure of zeolite NaY. MgO in form of magnesium nitrate is selected. The impregnation method was modified from McWilliams and co-workers (1988). The technique was used magnesium nitrate hexahydrate ($Mg(NO_3)_2·6H_2O$) in solution. After the calcination, it is decomposed into MgO, oxygen, and nitrogen oxides as the following equation (2-3) and the properties are shown in Table 2.2 (Gammon et al., 2007).

$$2Mg(NO_3)_2 \rightarrow 2MgO + 4NO_2 + O_2 \qquad\qquad (2\text{-}3)$$
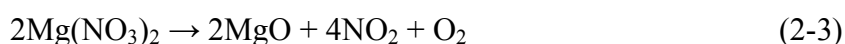
Table 2.2 $Mg(NO_3)_2 \cdot 6H_2O$ properties

IUPAC name	Magnesium nitrate
Molecular formula	$Mg(NO_3)_2 \cdot 6H_2O$
Molar mass	256.41 g/mol
Appearance	White crystalline solid
Density	2.3 g/cm^3 (anhydrous)
Melting point	88.9°C, hexahydrate
Boiling point	330°C
Solubility in water	125 g/100 mL
Electronegativity	1.31

2.5.3 Pelletization

Powder form of material causes a lot of pressure drop during the use. The pellet form is considered. Three methods for a pelletization including pressing, mechanical coating, and extrusion are interested in this study (McWilliams et al., 1988; Rahman et al., 1994; Yoshida et al., 2009).

2.5.3.1 Pressing

Pressing is the adsorbent compaction method involving uniaxial pressure applied to the powder placed in a die between two rigid punches as shows in Figure 2.7 (Rahman et al., 1994).
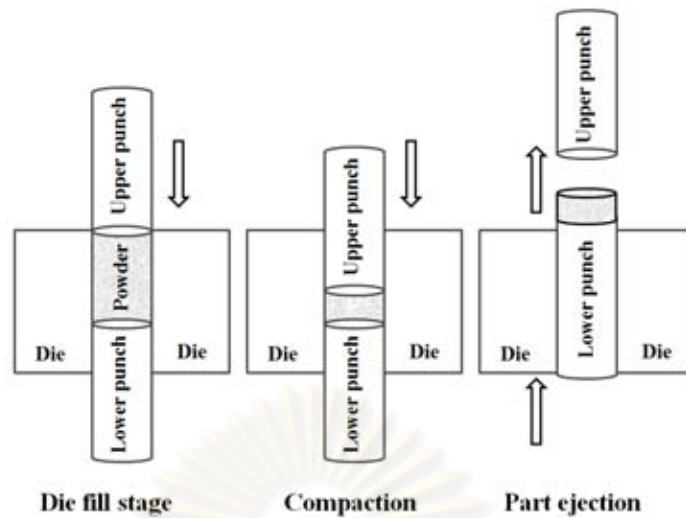
Figure 2.7 Pressing process (Rahman et al., 1994).

2.5.3.2 Extrusion

Extrusion is the adsorbent force passing through a die after mixed with inert binder, resulting in a long product (rods, bars, long plates, pipes) of regular cross-section, which may be cut into pieces of required length as shows in Figure 2.8 (McWilliams et al., 1988). Bentonite clay is used as binder in this study because it is inert material and not reacts with adsorbent. Bentonite has sodium in its structure which is one of required composition of zeolite NaY (Hughes, 1994).
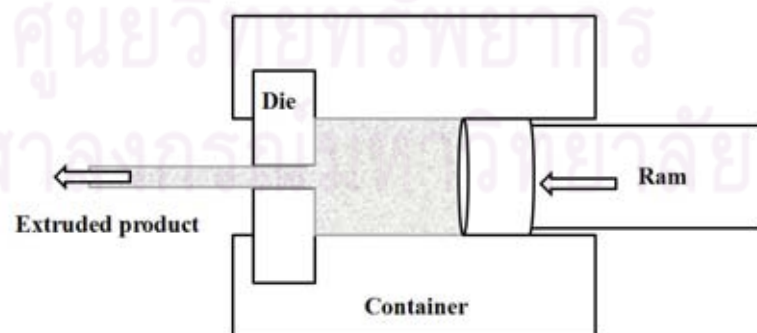
Figure 2.8 Extrusion process (McWilliams et al., 1988).

2.5.3.3 Mechanical coating

Mechanical coating is the adsorbent impacted with mechanic force from ball mill and coat on the ball as shows in Figure 2.9 (Yoshida et al., 2009).
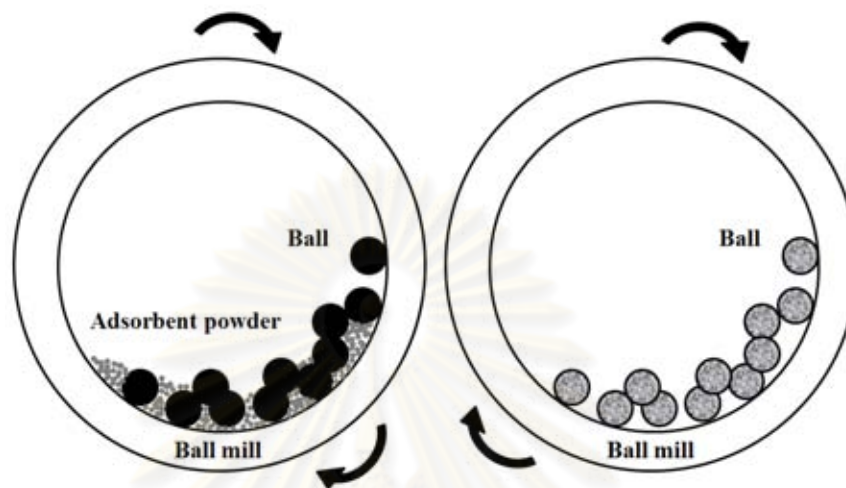
Figure 2.9 Mechanical coating process (Yoshida et al., 2009).

Adventages and disadventages of all three method in pelletization are listed in Table 2.3.

Table 2.3 Distinguishing of each pelletization method

Pelletization method	Advantages	Disadvantages
Pressing	Does not reduce the adsorption capacity	Does not use the binder that causes non-uniformity of particle size
Mechanical coating	Simple and produces uniform particle size	Eliminates the adsorption capacity
Extruding	Produces highly uniform particle size	Reduces the adsorption capacity with binder during the operation

CHAPTER III

METHODOLOGY

The experiment of this study is divided into two parts. The first part includes absorbent synthesis, pelletization and its characterization. In the second part, the adsorption study is explained, which includes column preparation, and HCl adsorption.

3.1 Material

3.1.1 Chemicals

The chemicals for extraction rice husk silica (RHS) were hydrochloric acid (37% HCl, Carlo-Erba), sodium aluminate (NaAlO$_2$, Sigma-Aldrich) and sodium hydroxide (NaOH, Carlo-Erba). RHS was obtained and used as a silica source for synthesis zeolite NaY. In the modification of adsorbent zeolite NaY, NaOH (Carlo-Erba) and both templates, hexadecyltrimethylammonium bromide (CTAB, Fluka) and poly diallydimethylammonium chloride (20% wt PDADMAC, Aldrich) were used. The metal salt for addition of positive charge was magnesium nitrate ((Mg(NO$_3$)$_2$·6H$_2$O, Fluka). The support for pelletization was alumina balls ranging in diameter of 1.2-2.0 mm. The HCl adsorption was studied under hydrogen gas 99.99% (H$_2$, Praxair) with the flow rate of 50 mL/min contaminated with 500 ppm hydrogen chloride gas (HCl, Thai Industrial Gas).

3.1.2 Instrument and apparatus

1) Basin with temperature controller for the reflux set
2) Furnace with temperature controller, with operating temperature up to 800°C
3) Filter-paper, Whatman number 1
4) Teflon-line autoclave

5) Polypropylene bottom

6) Filter-funnel

7) Reflux set; three-neck round bottom flask with condenser, heater (220 V, 1000W)

8) Vacuum pump

9) Stirrer and magnetic stirrer

10) pH tester-paper

11) Detector tubes number 14L (0-20 ppm) and 14M (0-500 ppm)

3.2 Experimental procedures

3.2.1 Silica extraction

Rice husk was refluxed with 3 M HCl for 3 h and washed with deionized water until the rinsed water was neutral. It was then dried at 100°C overnight and calcined in a furnace at 550°C for 6 h to remove organic impurities. The RHS was obtained and used as precursor for sodium silicate (Na_2SiO_3) preparation. 27 g of RHS was dissolved in 100 mL of 3.5 M NaOH solution to obtain a desired composition of Na_2SiO_3 for further zeolite NaY synthesis. The schemetic diagram of rice husk silica is shown in Figure 3.1.
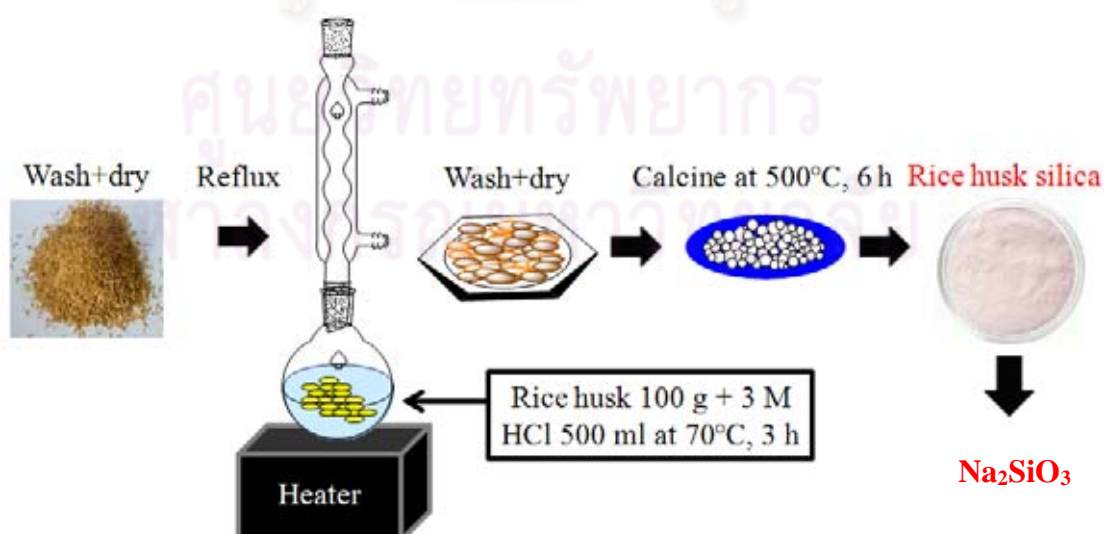
Figure 3.1 Synthesis of rice husk silica.

3.2.2 Preparation of zeolite NaY

The zeolite NaY was synthesized by a hydrothermal method, the seed gel and the feedstock gel were prepared. The seed gel in molar composition of $4.30Na_2O:Al_2O_3:10SiO_2:180H_2O$ was prepared by dissolving 4.09 g of NaOH and 2.09 g of $NaAlO_2$ with 20 mL of deionized water before addition of 27.72 g of Na_2SiO_3 solution and then aging at room temperature for 1 day. The feedstock gel in molar composition of $10.67Na_2O:Al_2O_3:10SiO_2:180H_2O$ was prepared by dissolving 0.14 g of NaOH and 13.09 g of $NaAlO_2$ with 130 mL of deionized water before addition of 142.43 g of Na_2SiO_3 solution but without aging. After that, the both gels were mixed and crystallized at 90°C for 22 h, the solid product was washed several times until pH < 10 and dried at 100°C. The synthesis zeolite NaY diagram is shown in Figure 3.2.

Figure 3.2 Synthesis of zeolite NaY.

3.2.3 Preparation of Meso-NaY

The Meso-NaY was prepared by two methods including leaching and adding templates. The obtained zeolite NaY was used as precursor. The leaching, 30 mL of 0.2 M NaOH was used in 1 g of zeolite NaY for 30 min (Abello et al., 2009). For the addition templates, the templates were added during mixing both gels of NaY synthesis with molar composition of $4SiO_2:1CTAB$ and $2562SiO_2:1PDADMAC$ (Liu et al., 2008; Saporm, 2005). The obtained Meso-NaY by adding templates was

characterized with Thermogravimetric analysis technique (TGA) to find suitable temperature for calcination temperature. The Meso-NaY which has highest HCl adsorption capacity was used as a support for Mg loading study. The synthesis of Meso-NaY pattern is presented in Figure 3.3.

a) Meso-NaY(Leaching)

b) Meso-NaY(Templates)
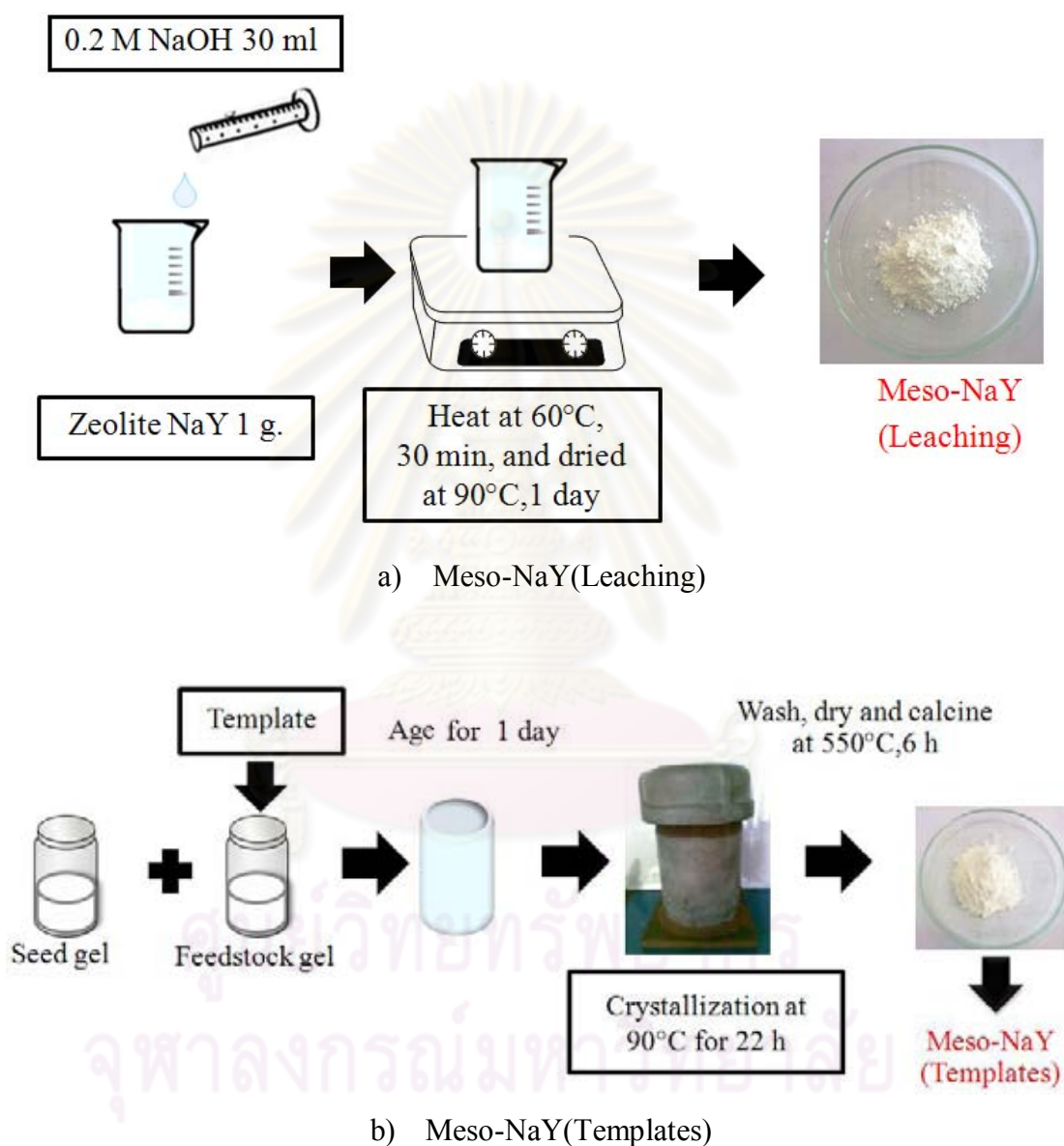
Figure 3.3 Synthesis of Meso-NaY:

a) Meso-NaY (Leaching); b) Meso-NaY (Templates).

3.2.4 Preparation of Mg/Meso-NaY

Mg/Meso-NaY was prepared by impregnation method (Abllo et al., 2009), with $Mg(NO_3)_2 \cdot 6H_2O$ solution (5%wt of Mg). The resulting wetted solid was dried and calcined at 300°C for 3 h. The Mg-Meso-NaY was obtained and used as an adsorbent for HCl adsorption. The synthesis of Mg/Meso-NaY diagram is presents in Figure 3.4.
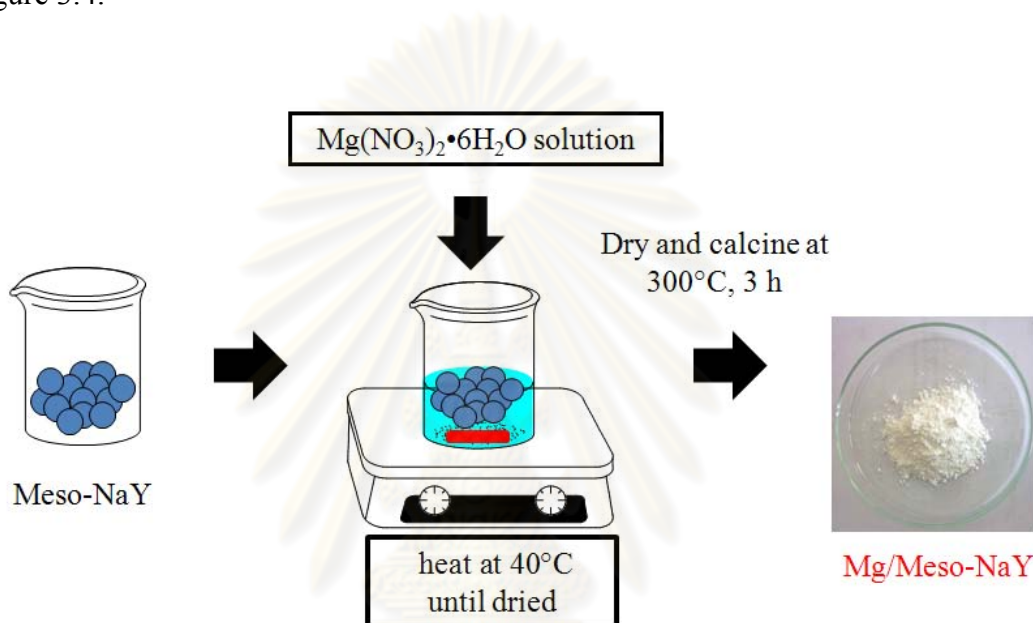
Figure 3.4 Synthesis of Mg/Meso-NaY.

3.2.5 Characterization

The physical and chemical properties of the studied adsorbent were examined by X-ray Diffraction (XRD), nitrogen adsorption-desorption isotherms, Fourier Transform Infrared (FTIR), Scanning Electron Microscopy (SEM), and X-ray Fluorescence (XRF) as follows;

The XRD patterns and the crystallinity structures of adsorbent were obtained by XRD spectrometer (BRUKER AXS: D8 ADVANCE A25) with CuKα 40kV, 40 mA. The scanning was performed at 2θ radiation in regular range from 5° to 60° for all of absorbent. The mean crystallite sizes of samples were evaluated by the Scherer equation (3-1):

$$D = \frac{k\lambda}{\beta\cos\theta} \quad \ldots\ldots\ldots\ldots\ldots\ldots\ldots\ldots\ldots\ldots\ldots(3\text{-}1)$$

Where λ is 1.54 corresponding to irradiation wavelength, k is 0.9, β is the full width at half maximum of strongest line and θ is the Bragg angle of the most intense peak at a specific phase.

The functional groups of adsorbent were studied by BRUKER TENSOR27. 1 mg of sample is mixed with 100 mg of KBr and ground. Then, the sample was pressed to make the pellets at 10 bar. The wave number was scanned in the region of 4000 to 400 cm^{-1}.

The nitrogen adsorption-desorption isotherms at -196ºC in relative pressure (P/P_0) range of 0.01-0.99 of the adsorbent were measured with a Autosorb-1 chrantachrome, BL model. The surface areas were calculated by applying the Brunauer-Emmet-Teller (BET) equation.

The surface morphology of samples was examined by SEM, using a Jeol scanning microscope model JSM-5410 operated at 15 kV. Powder samples were sprinkled uniformly over an adhesive tape and sputter coated with gold by sputter coater, prior to admission into the microscope.

The composition of spent adsorbent was measured by X-ray Fluorescence (Philips PW 2400).

3.2.6 Pelletization of adsorbent

The adsorption study used the adsorbent in form of beads. The pelletization of adsorbent in this study was in three methods including pressing, mechanical coating, and extrusion.

3.2.6.1 Pressing

The adsorbent was pressed by pressurized pellelizator under condition 3 bar for 2 min. The adsorbent in pellet form was obtained in cylinder shape with depth of 1 cm. The obtained adsorbent was crashed to smaller size and sieved with 2 mm molecular sieves. The final pelleted adsorbent was shown in Figure 3.5.

Figure 3.5 Pellet form by pressing method.

3.2.6.2 Extrusion

The adsorbent was extruded by mixing with an inert binder. The properties of an inert binder are similar with the adsorbent and inactive with the adsorbent. The bentonite clay in molar ratio of $Al_2O_3 \cdot 4SiO_2 \cdot 2H_2O$ was applied as binder in this study. The swollen bentonite clay was sticky after adsorbed water. In this study, the varying ratio of adsorbent and bentonite clay was 7:3, 8:2 and 9:1 for finding the suitable and less amount of binder. The bentonite clay was mixed with adsorbent before extruded with a syringe. Then, the obtained long cylindrical shape adsorbent was cut and sieved to the size of 2 mm as shown in Figure 3.6. and 3.7

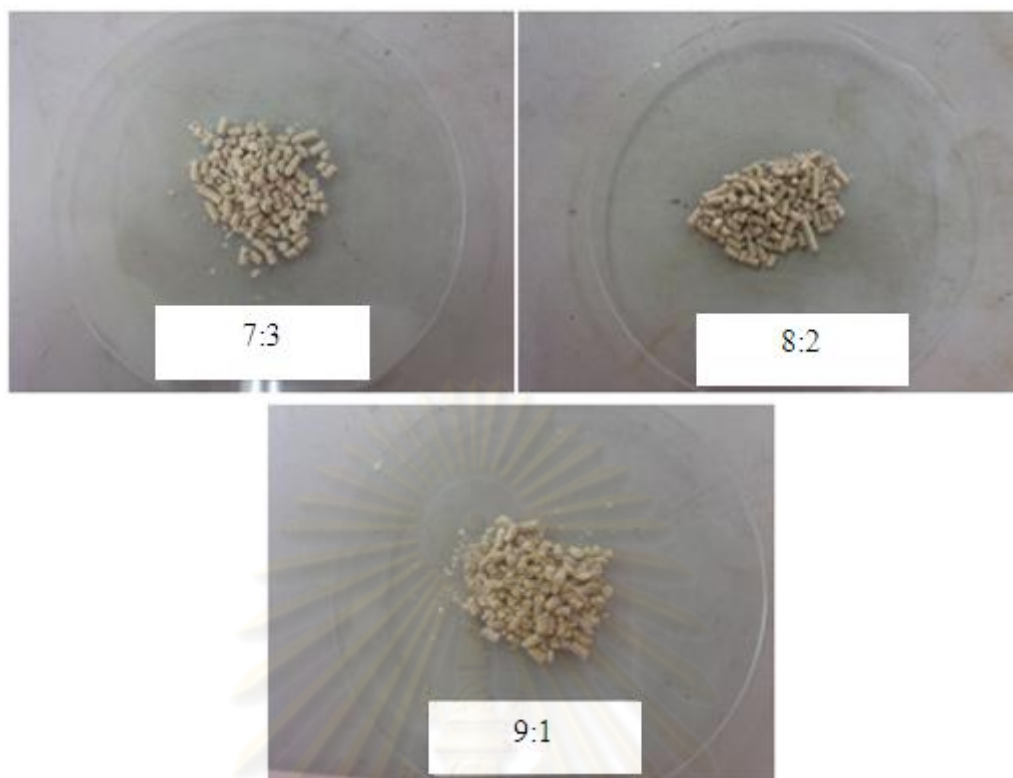**Figure 3.6** Bentonite clay in pellet form.

Figure 3.7 Pellet form by bentonite in different ratios.

3.6.2.3 Mechanical coating

The powder adsorbent and alumina ball of 1.2-2.0 mm size were mixed in ratio 4:6 and rotated in milling machine for 24 h. After that, it was calcined at 550°C for 6 h. The obtained adsorbent is shown in Figure 3.8.

Figure 3.8 Adsorbent with mechanical coating.

3.2.7 HCl adsorption

Adsorption performances of studied adsorbents were carried out in a continuous packed-bed column. The column of 1 cm diameter was constructed with glass. Approximately 1 g of studied adsorbent was packed in 3 layers alternated with quartz wool. Each layer was packed in 2 cm high. Feed gas with major component of H_2 contaminated with 500 ppm HCl. was flowed into the column with feed rate of 50 mL/min. as shows in Figure 1. Effluent from the adsorption column was measured using special gas detector tube No. 14L-14M for HCl. Detection limits for each gas detector tube are 0.05 ppm. The all adsorbents were used for HCl removal compared with commercial. The bed capacity of HCl adsorption was calculate by equation (3-2 to 3-4). The chloride quantity in spent adsorbent was also confirmed by XRF.

$$W_{sat} = \frac{F_A \text{ x Area above the breakthrough curve graph}}{\text{Mass of adsorbent per unit cross section area of bed}} \quad \dots\dots\dots\dots(3\text{-}2)$$

$$W_b = \frac{F_A \text{ x Area above the breakthrough curve graph at breakpoint}}{\text{Mass of adsorbent per unit cross section area of bed}} \quad \dots\dots(3\text{-}3)$$

$$\text{Bed capacity} = \frac{W_b}{W_{sat}} \quad \dots\dots\dots\dots\dots\dots\dots\dots\dots(3\text{-}4)$$

where W_{sat} is adsorption potential ($g_{HCl}/g_{adsorbent}$); W_b is adsorption potential when C/C_0 is the concentration in fluid relative to that in feed (Breakpoint: $C/C_0 = 0.05^*$) and F_A is the feed rate of solution ($g(cm^2/h)$)The HCl adsorption is studied at the end of each synthesis adsorbent that includes Meso-NaY and Mg-Meso-NaY, the adsorbent were placed in the column. The experiment scheme is shown in Figure 3.10.
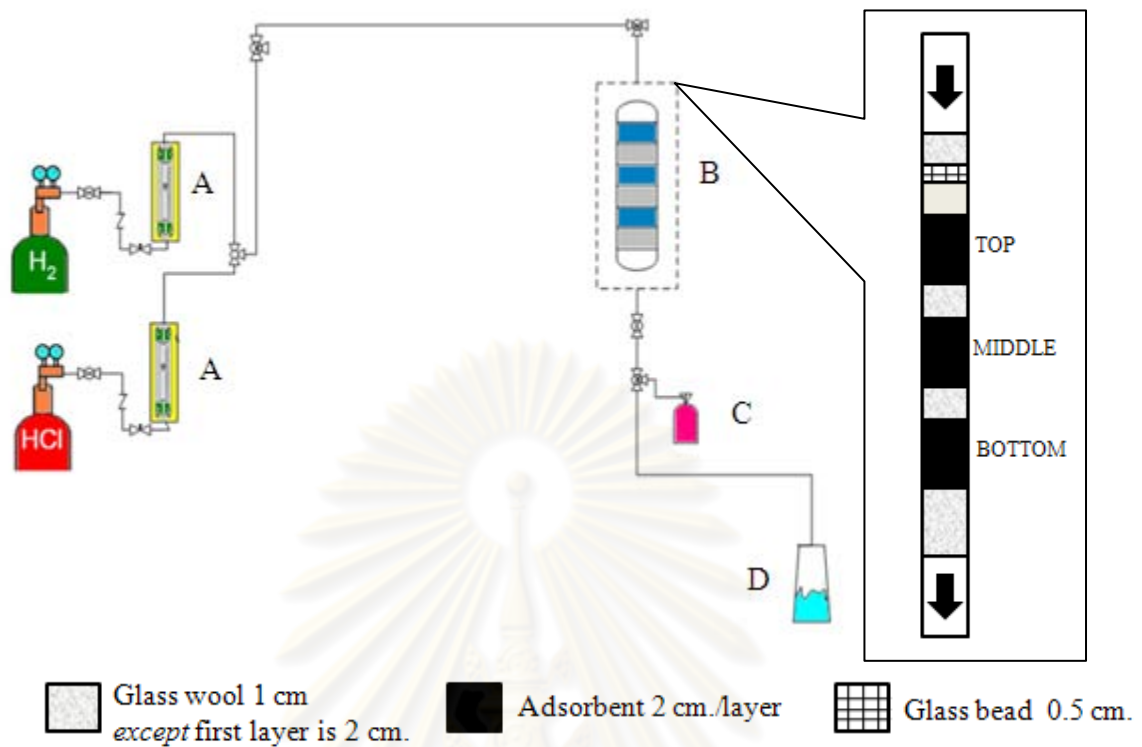
Figure 3.9 Fixed-bed flow adsorption reactor.

* Breakpoint: $C/C_0 = 0.05$ is relative concentration at breakpoint which usually of 0.05. The flow should stop or divert to fresh adsorbent.
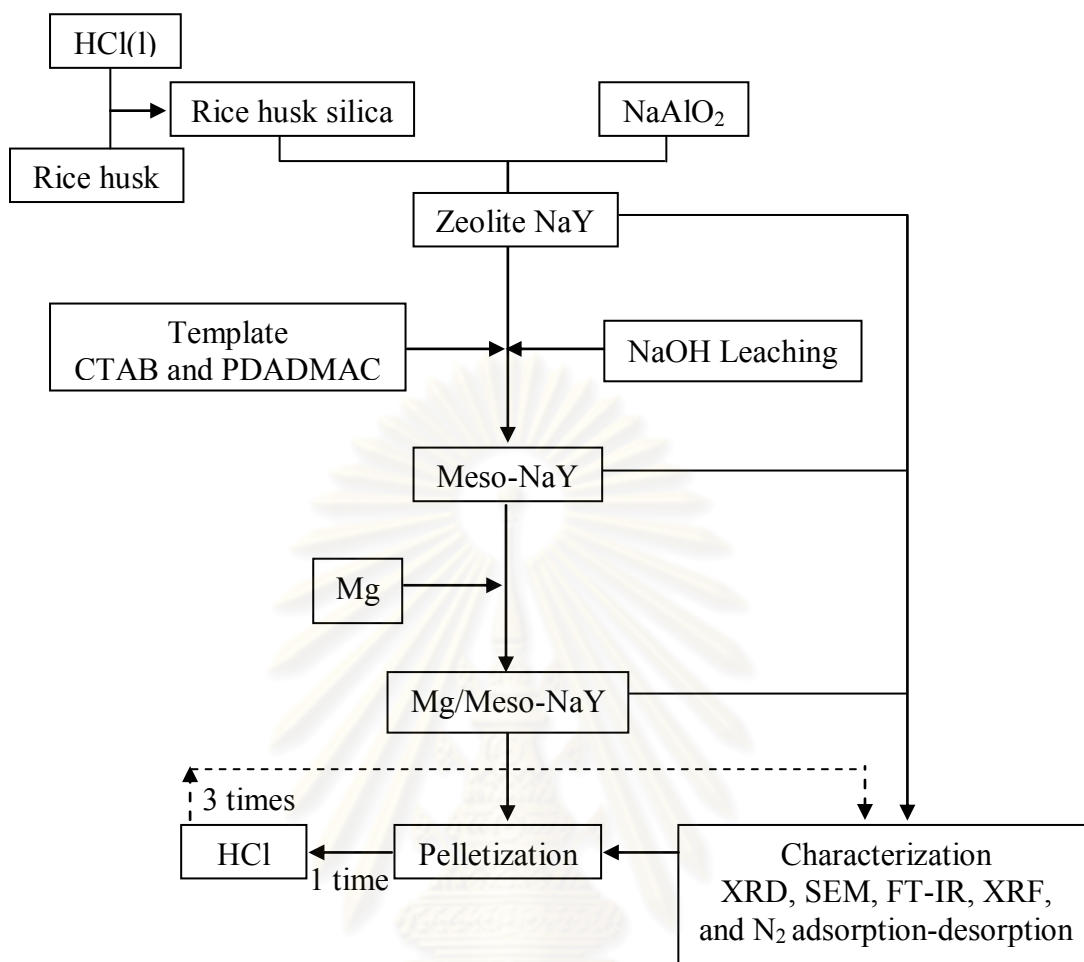
Figure 3.10 Schematic diagram of experiment.

ศูนย์วิทยทรัพยากร
จุฬาลงกรณ์มหาวิทยาลัย

CHAPTER IV

RESULTS AND DISCUSSION

4.1 Characterization

4.1.1 Rice husk silica

The XRD pattern of rice husk silica is shown in Figure 4.1. Only a broad peak at 22º was observed indicating that the phase of rice husk silica was amorphous. This phase was suitable for preparation of sodium silicate for synthesis of zeolite NaY because this phase easily dissolved in sodium hydroxide solution. Generally, zeolite NaY using silica form rice husk ash required the calcination tempareture at 700ºC. It was suggested to use long period of ageing time possible due to the low which was possible a long crystalline. (Kordotos et al., 2008).

Figure 4.1 XRD pattern of rice husk silica.

4.1.2 As-synthesized Meso-NaY

Silica obtained from rice husk was utilized from sodium silicate. It was readily as a precursor of Meso-NaY zeolite preparation. Since two chemicals (CTAB and PDADMAC) were used as a template in the Meso-form synthesis part, it was required to find out the suitable calcination temperature. TGA and DTA profiles of as-synthesized Meso-NaY are characterized, as shown in Figure 4.2.
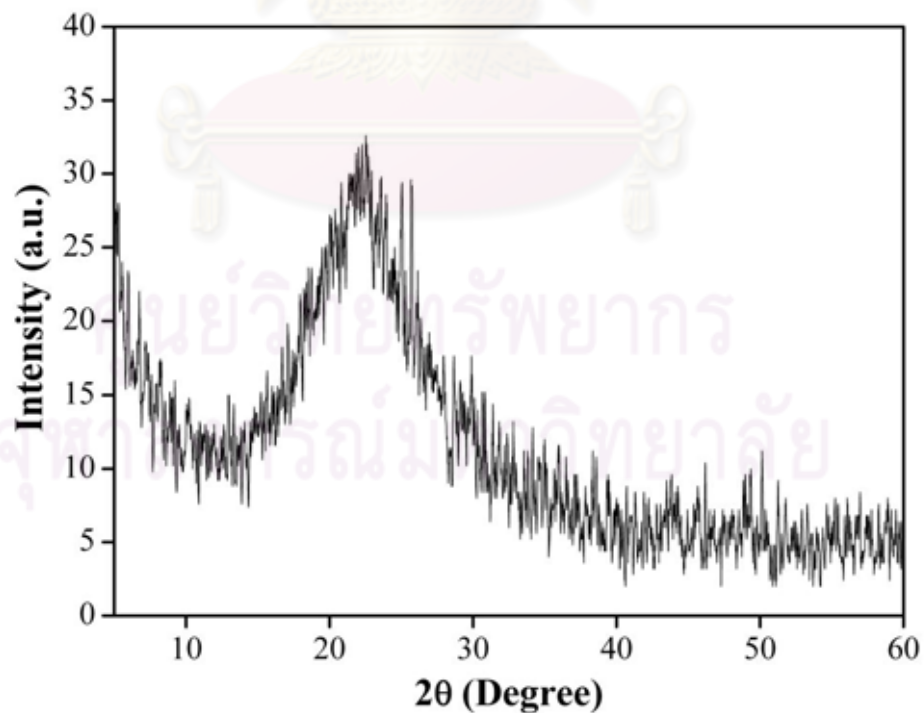
Both of CTAB and PDADMAC templates showed the similar results. The initial weight loss which was observed at temperature less than 200ºC caused by the desorption of physically adsorbed water. The main weight loss could be observed in the temperature range of 200-500ºC. It was assigned to the organic template decomposition. The weight loss above 500ºC was related to water loss from condensation of adjacent Si-OH groups to siloxane bond (Si-O-Si). Therefore, the calcination temperature for organic template removal in this work was 550ºC. The weight losses beyond 500°C in both TGA profiles seemed to be constant. In this range of temperature, the DTA peaks were observed. To ensure the suitable temperature to remove organic templates, it is better to extend for higher temperature of further study. Therefore, 550°C was selected for calcination temperature, which was similar to Liu et al.'s work (2008).
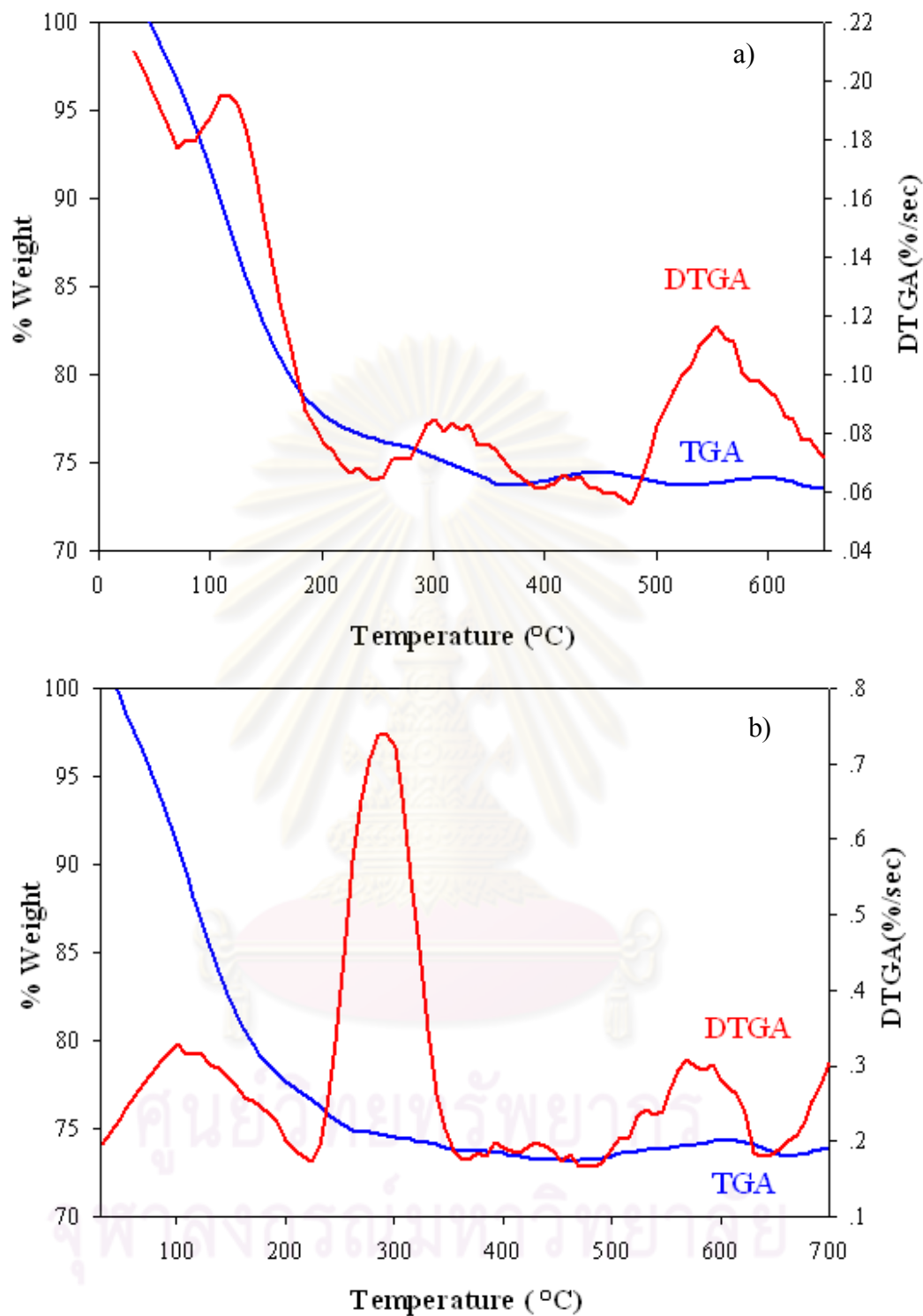
Figure 4.2 TGA and DTA profiles of the as-synthesized adsorbents using
a) Meso-NaY (CTAB) and b) Meso-NaY (PDADMAC).

Obtained NaY and Meso-NaY were analyzed through XRD compared to standard pattern of zeolite NaY, as presented in Figure 4.3. As seen, all prepared

XRD patterns had similar pattern to the standard zeolite NaY pattern. After modification, the characteristic peaks of Meso-NaY indicated that the structure of Meso-NaY was not changed.

From the XRD patterns, crystallite size of each material is calculated from Scherrer equation. The results of crystallite size are tabulated in Table 4.1. Meso-NaY showed larger crystallite size compared to original NaY, after structure destroying by leaching and templates.

Figure 4.3 XRD patterns of synthesis zeolite NaY and Meso-NaY.

Table 4.1 Crystallite sizes of standard zeolite NaY, zeolite NaY, and Meso-NaY

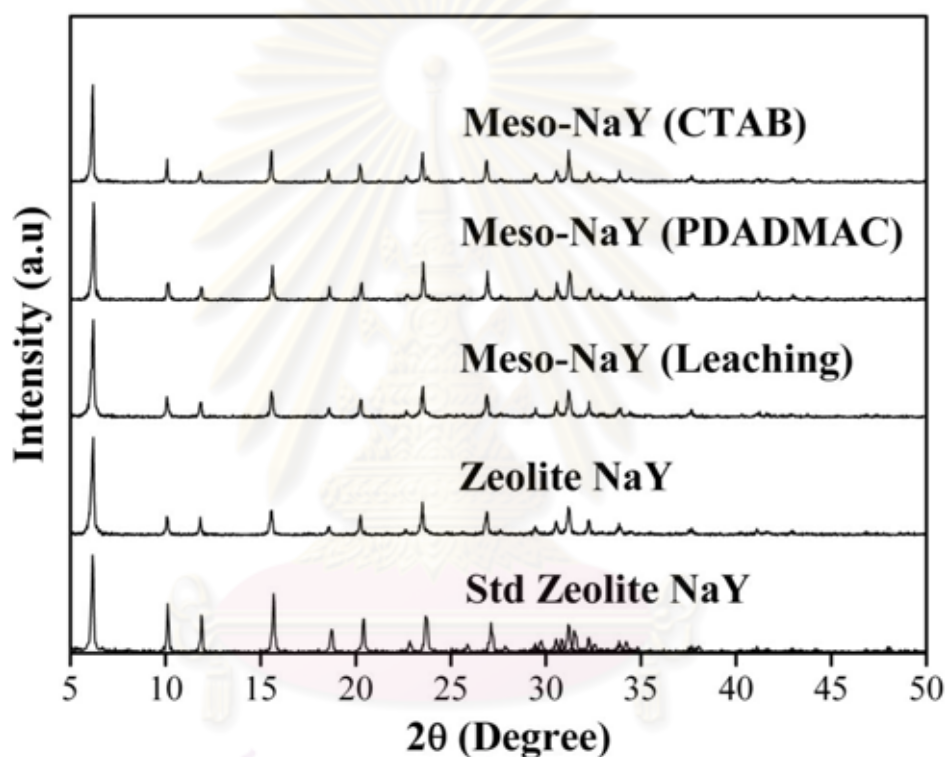| Adsorbent	Crystallite size (nm)
Standard zeolite NaY	1.1547
Zeolite NaY	0.7720
Meso-NaY (Leaching)	0.8685
Meso-NaY (CTAB)	1.1540
Meso-NaY (PDADMAC)	1.5440

The morphology of synthesis zeolite NaY and Meso-NaY by SEM technique is shown in Figure 4.4. Figure 4.5 shows the size distribution of all studies zeolite NaY. The particles of zeolite NaY and Meso-NaY (Templates) look like octahedral and twinned approximately in the range of 1.4-1.7 μm and 1.1-1.4 μm, respectively. Most of particle of Meso-NaY (Leaching) was twinned in the range of 2.11-2.40 μm. Meso-NaY (Leaching) was larger than Meso-NaY (Template). Consequently, each crystal was leached by NaOH solution to produce smaller size afterward the small crystal agglomerated to form large particle. Meanwhile, template played a great role in structural material for synthesis and produce uniform particles while particle of zeolite NaY might be fused to larger size (Liu et al., 2008).
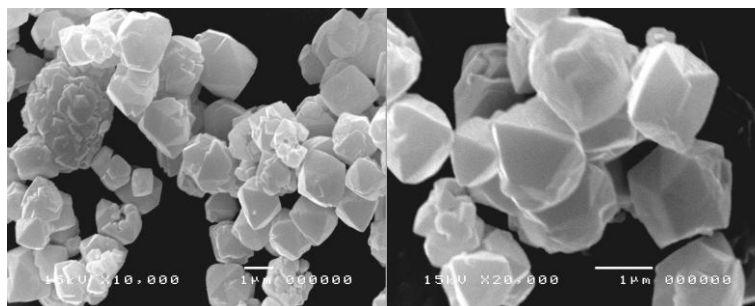
a)   Zeolite NaY
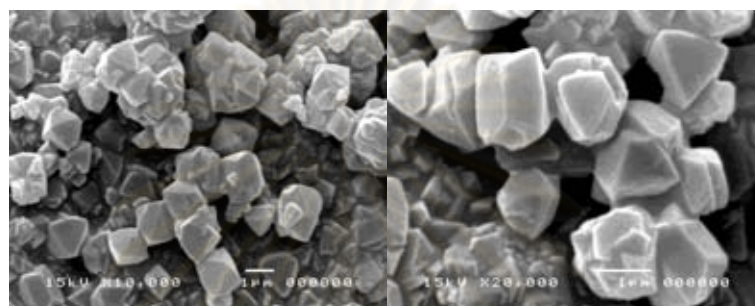
b)   Meso-NaY (Leaching)
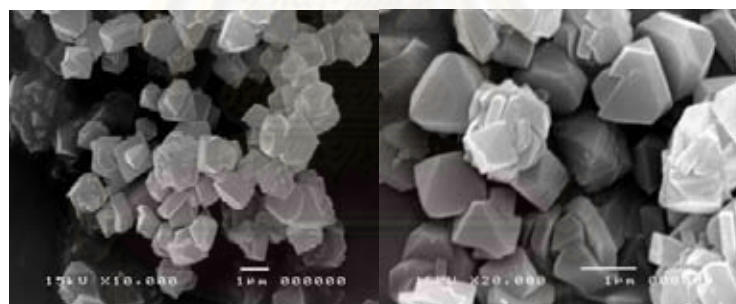
c)   Meso-NaY (CTAB)
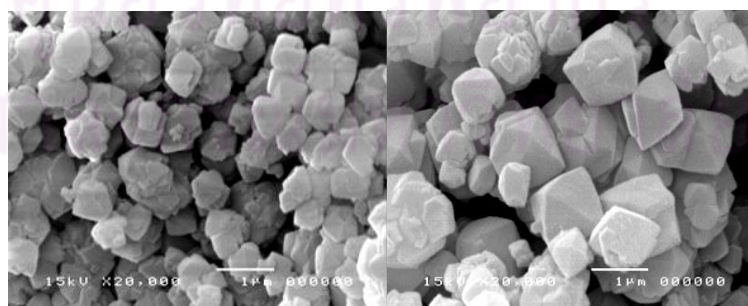
d)   Meso-NaY (PDADMAC)

Figure 4.4 SEM images of Na and Meso-NaY at 10k (left) and 20k (right).
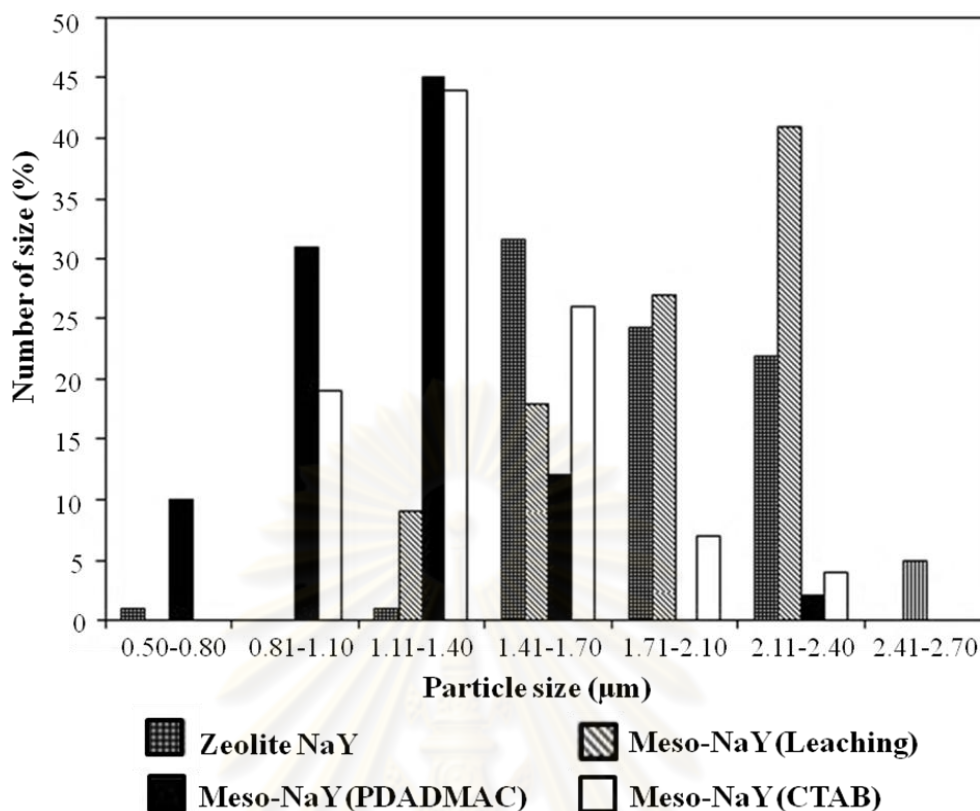
Figure 4.5 Particle size distribution of Meso-NaY.

The N_2 adsorption-desorption isotherms of zeolite NaY and Meso-NaY are plotted compared with zeolite NaY, as shown in Figure 4.6. All isotherms presented type I typical for microporous material similar with Liu's work (Liu et al., 2008). However, the hysteresis loop was presented at relative pressure (P/P_0) for Meso-NaY. This indicated that the mesopore were generated in the Meso-form. This results confirmed that Meso-NaY possesed both micropores and mesopores. Therefore, the surface area and the pore volume of Meso-NaY were increased 1.2 times and 1.1 times, respectively as shown in Table 4.2. The Meso-NaY (PDADMAC) and Meso-NaY (Leaching) was selected to characterize by Scanning Electron Microscope-Energy Dispersive X-ray spectroscopy technique because its surface area is high. Since the properties of Meso-NaY (CTAB) are expensive and use in large amount.
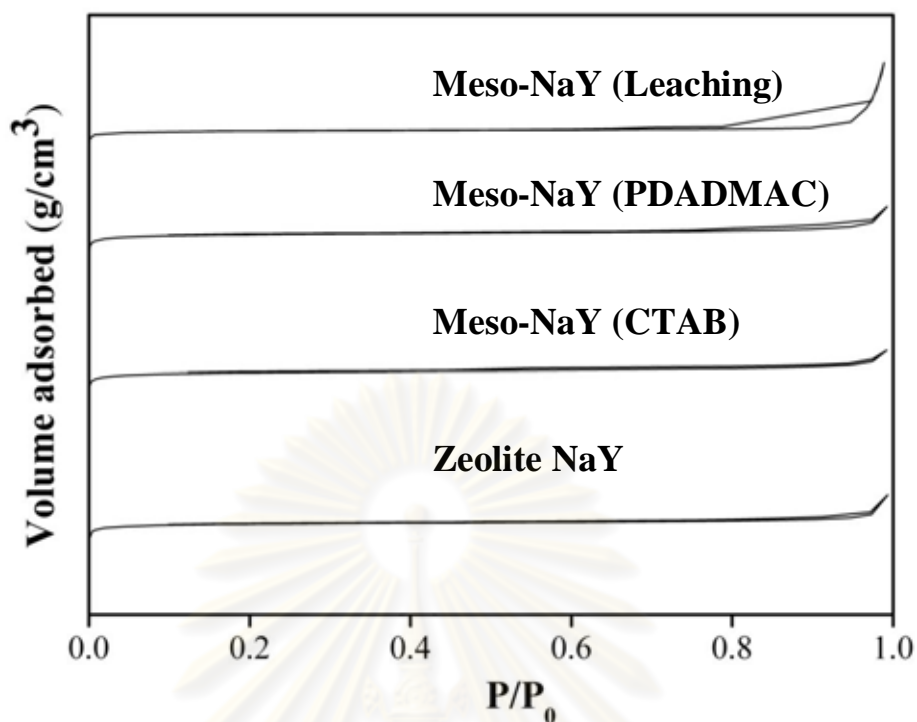
Figure 4.6 Adsorption-desorption isotherms of synthesis adsorbents.

Table 4.2 Surface areas and pore volumes of zeolite NaY and Meso-NaY

Sample	Surface area (m^2/g)	Total pore volume (cm^3/g)
Commercial	180	-
Zeolite NaY	533	0.3302
Meso-NaY (CTAB)	514	0.3021
Meso-NaY (PDADMAC)	605	0.3144
Meso-NaY (Leaching)	653	0.5889

The SEM-EDS results of NaY-zeolite and Meso-NaY (Leaching) and Meso-NaY (PDADMAC) show the dispersion of metals in samples of main components (Na, Al and Si) (Figure 4.7). It was found that each metal was well dispersed on the adsorbents and it caused higher efficiency in the gas adsorption. Additional the Na content of Meso-NaY (Leaching) compared with that of zeolite NaY was quite higher. Therefore, Meso-NaY (Leaching) was selected to characterize by FTIR technique.
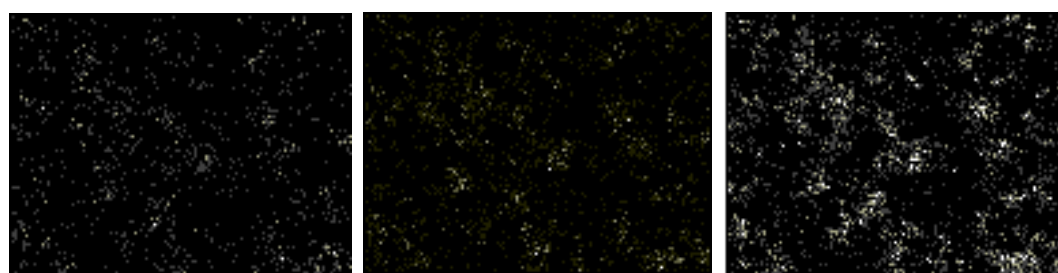
a)   NaY (Na)   b) NaY (Al)   c) NaY (Si)
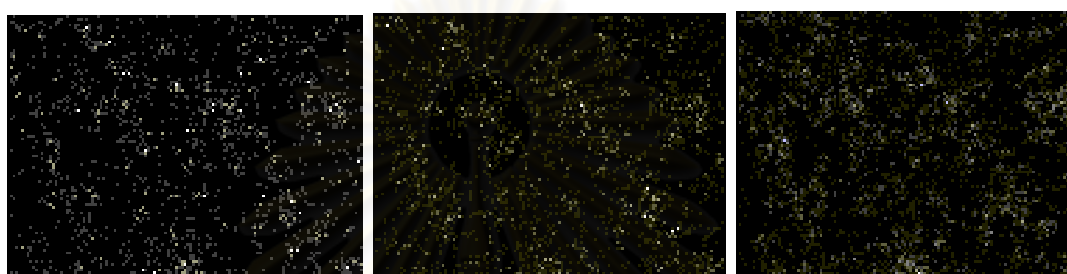
a) Meso-NaY (Leaching) (Na) b) Meso-NaY (Leaching) (Al) c) Meso-NaY (Leaching) (Si)

a) Meso-NaY (PDADMAC) (Na) b) Meso-NaY (PDADMAC) (Al) c) Meso-NaY (PDADMAC) (Si)

Figure 4.7 Dispersion of element composition on zeolite NaY and Meso-NaY.

FTIR spectrum of Meso-NaY (Leaching) presents peaks at 3450 cm^{-1}, 1025 cm^{-1}, 578 cm^{-1} and 456 cm^{-1} (Figure. 4.8). According to the peaks that appeared at 3435 cm^{-1} is assigned to the O-H stretching vibration mode of hydroxyl functional groups. The appearance peaks at 1025 cm^{-1} and 456 cm^{-1} are assigned to tetrahedral vibration. The band around 578 cm^{-1} is referred to the double ring external linkage peak associated with FAU structure (Rahman et al., 2009; Sang et al., 2006).
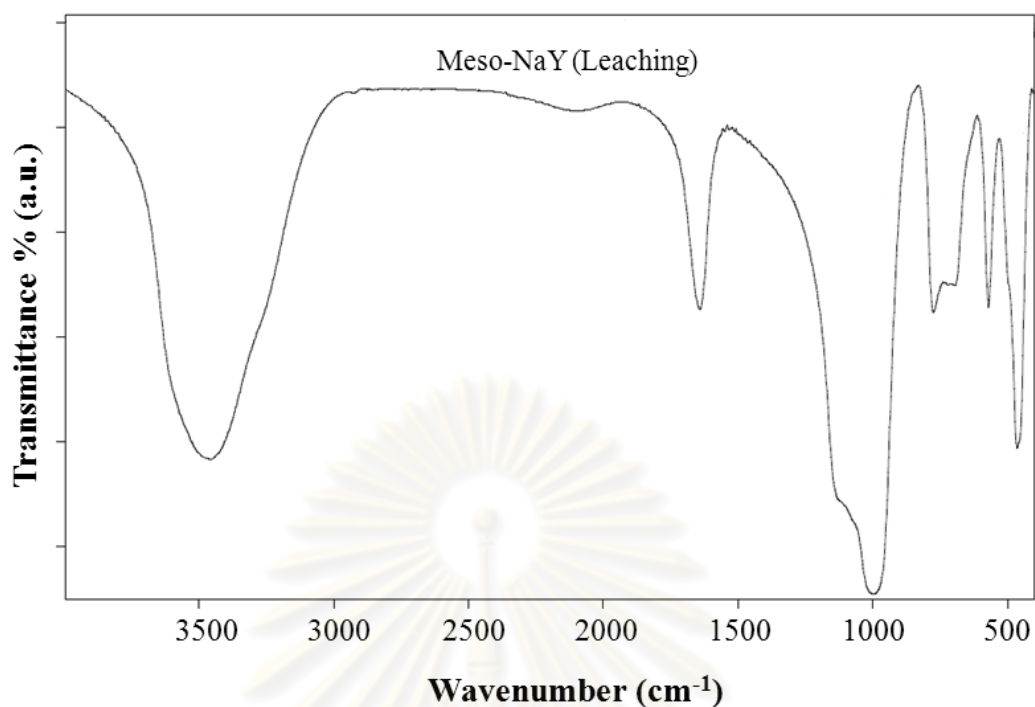
Figure 4.8 FTIR spectrum of Meso-NaY (Leaching).

4.2 HCl adsorption study

The HCl adsorption is studied in fixed-bed flow reactor under H_2 feed rate of 50 mL/min contaminated with 500 ppm.

4.2.1 Meso-NaY performance

The adsorbent beads were packed in the column and tested in a fixed-bed flow reactor. Meso-NaY (Leaching) showed greater in adsorption potential ($W_b = 0.2355$ $g_{HCl}/g_{adsorbent}$) than zeolite NaY ($W_b = 0.1046$ $g_{HCl}/g_{adsorbent}$), Meso-NaY (PDADMAC g_{HCl}/g $g_{adsorbent}$) ($W_b = $ $g_{HCl}/g_{adsorbent}$) and commercial ($W_b = 0.0819$ $g_{HCl}/g_{adsorbent}$) as shown in Table 4.3. Consequently, Meso-NaY (Leaching) has high surface area and large amount of Na according to the result of BET surface area and SEM-EDS that has mentioned. However, The surface of commercial is low but its adsorption potential is almost equal to synthesized zeolite NaY that indicated the Na

content was main factor that affected to adsorption potential. Therefore, Meso-NaY (Leaching) was further used to apply in addition of positive charge.
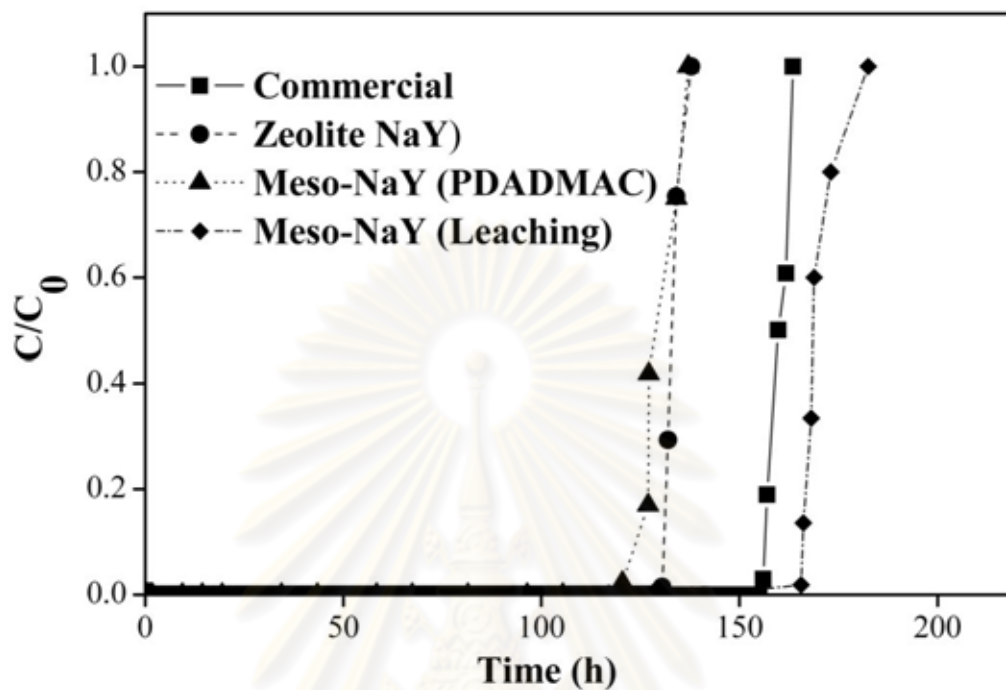
Figure 4.9 HCl breakthrough curves on commercial and synthesis adsorbents.

Table 4.3 Adsorption capacity of HCl on zeolite NaY, and Meso-NaY

Adsorbents	W_{sat} (g_{HCl}/g^*)	W_b (g_{HCl}/g^*)	Bed Capacity
Commercial	0.0838	0.0819	0.9773
Zeolite NaY	0.1012	0.1046	0.9613
Meso-NaY (Leaching)	0.2359	0.2355	0.9477
Meso-NaY (PDADMAC)	0.1076	0.1027	0.9545

*g is weight of adsorbents

4.2.2 Mg/Meso-NaY performance

The XRD patterns of Meso-NaY (Leaching) and Mg/Meso-NaY (Leaching) are shown in Figure 4.10. In the modified material, the peaks representing Meso-NaY remained the same. It indicated its structure was not changed after addition of positive charge into Meso-NaY (Leaching). However, the surface area of Mg/Meso-NaY (Leaching) (175 m^2/g) was decreased dramatically (more than half of its surface area) when compared to that of Meso-NaY (Leaching) (589 m^2/g). The surface area of the adsorbent should be taken into discussion. The surface area particular the pores, of Mg/Meso-NaY (Leaching) was blocked by Mg. This observation was agreed with the report by Park and Jin's work (2003).
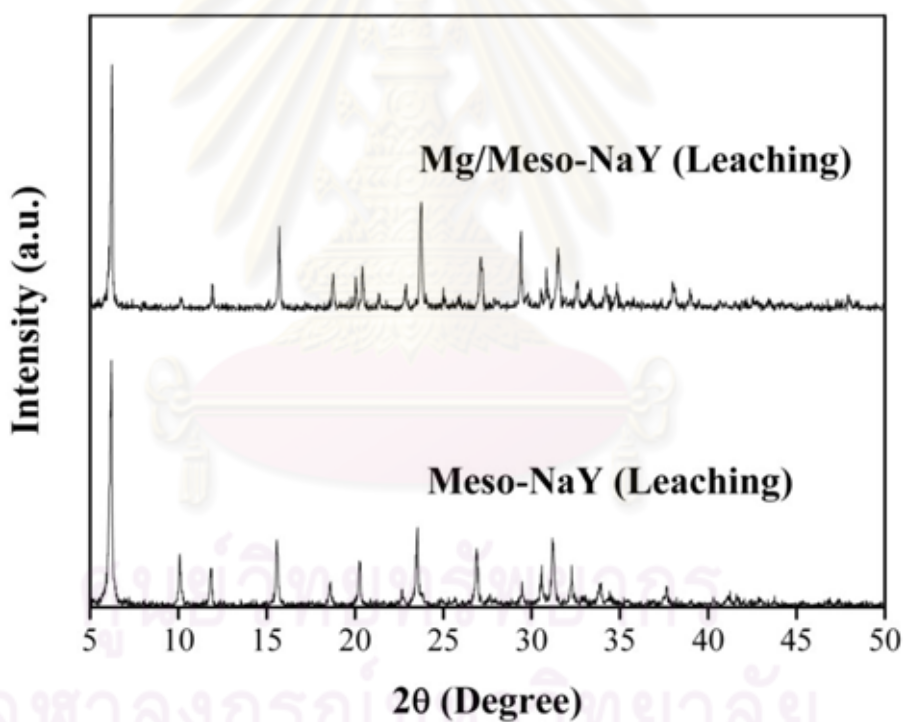
Figure 4.10 XRD patterns of Meso-NaY (Leaching) and Mg/Meso-NaY (Leaching).

Table 4.4 Surface areas of Meso-NaY (Leaching) and Mg/Meso-NaY (Leaching)

Samples	Surface area (m^2/g)
Meso-NaY (Leaching)	653
Mg/Meso-NaY (Leaching)	175

The HCl adsorption potential of modified Meso-NaY by addition of positive charge on structure of Meso-NaY (Leaching) is lower than that of Meso-NaY from NaOH-leaching method, as shown in Figure 4.11. The adsorption calculations were listed in Table 4.5. Thus, the qualities of a good adsorbent for HCl adsorption should have high surface area and contain large amount of active metal. Moreover, Meso-NaY (Leaching) was selected to study in pelletization for investigation the effect of shape.
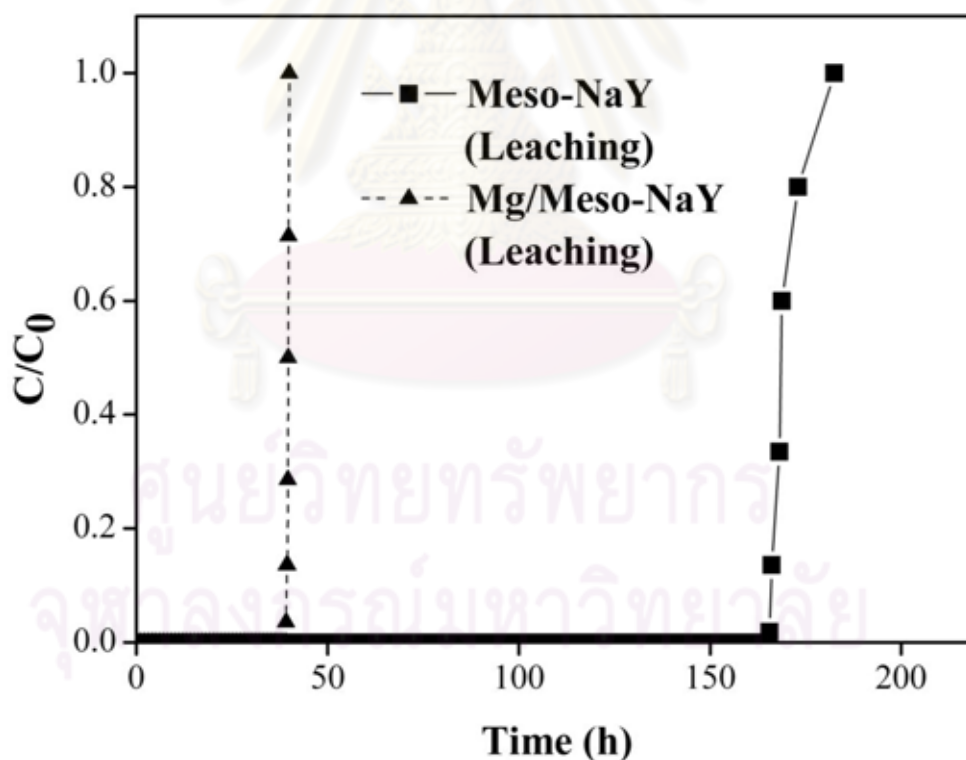

Figure 4.11 HCl breakthrough curves on Meso-NaY (Leaching)
and Mg/Meso-NaY (Leaching)

Table 4.5 Adsorption capacity of HCl of Meso-NaY (Leaching) and

   Mg/Meso-NaY (Leaching)

Adsorbent	W_{sat} (g_{HCl}/g^*)	W_b (g_{HCl}/g^*)	Bed Capacity
Meso-NaY (Leaching)	0.2359	0.2355	0.9477
Mg/Meso-NaY (Leaching)	0.0463	0.0463	0.9995

*g is weight of adsorbents

4.3 Pelletization study

   The BET surface area of Meso-NaY (Leaching), Meso-NaY (Leaching) in pellet form supporter and binder are presented in Table 4.6. The surface area of Meso-NaY (Leaching) in pellet form by pressing and extrusion were slightly decreased. Meanwhile, the surface area Meso-NaY (Leaching) by Mechanical coating was decreased almost 30%. Pressing method, the pore of Meso-NaY (Leaching) was pressed due to pressurized. The composition of Meso-NaY (Leaching) of both extrusion and mechanical coating were not only Meso-NaY (Leaching) but also bentonite clay as the binder and alumina ball as the media, respectively. This would be a reason why surface area of obtained Meso-NaY (Leaching) in pellet form was decreased.

Table 4.6 BET surface areas of Meso-NaY (Leaching) in pellet form

Adsorbents	Pelletization methods	Surface area (m^2/g)
Meso-NaY (Leaching)	Pressing	643
	Extrusion (Mixing with binder)	593
	Mechanical coating	188
Supporter	Alumina ball	307
Binder	Bentonite clay	95

The HCl adsorption potential of Meso-NaY (Leaching) from pressing method was higher than that of Meso-NaY from other methods as shown in Figure 4.12 and Table 4.7. According to the result of BET surface area, its surface area is highest. Therefore, Meso-NaY (Leaching) in pellet form by pressing was selected for repetitions in HCl adsorption to confirm its HCl adsorption capacity.
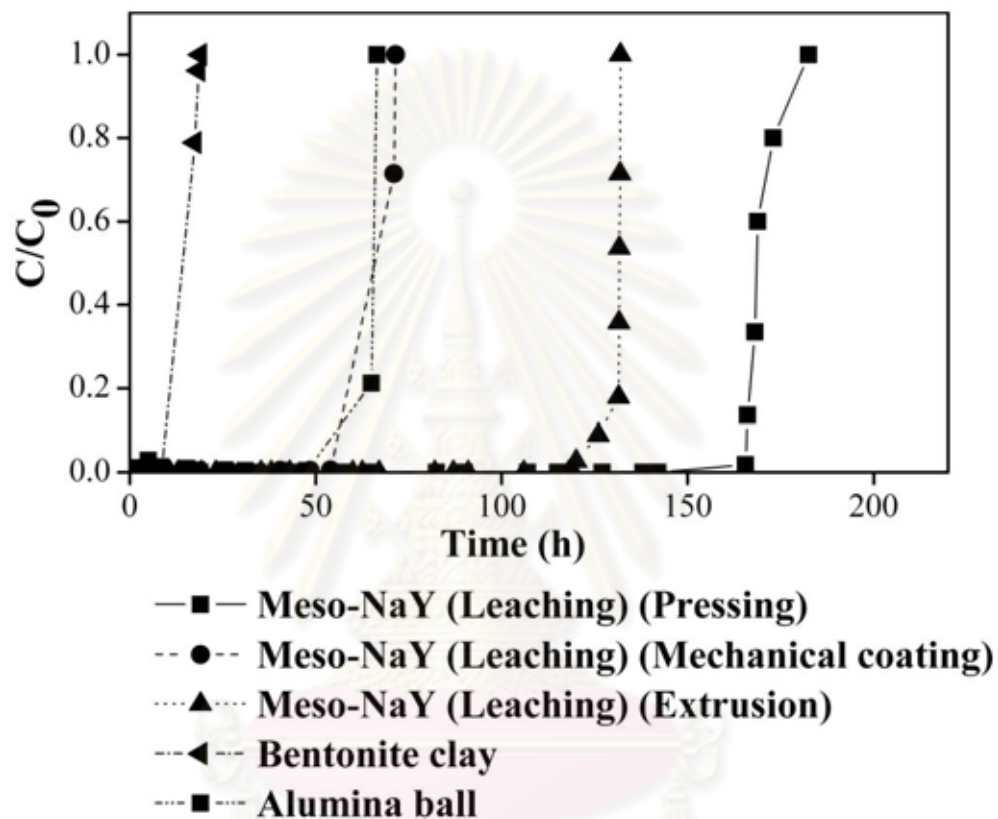
Figure 4.12 HCl breakthrough curves on Meso-NaY (Leaching) in pellet forms.

Table 4.7 Adsorption capacity of Meso-NaY (Leaching) in pellet forms

Adsorbents	W_{sat} (g_{HCl}/g^*)	W_b (g_{HCl}/g^*)	Bed Capacity
Meso-NaY (Leaching)			
-Pressing	0.2359	0.2355	0.9984
-Extrusion	0.1212	0.1132	0.9309
-Mechanical	0.1855	0.1587	0.9133
Alumina ball	0.0608	0.0450	0.7046
Na-bentonite clay	0.0046	0.0071	0.6551

*g is weight of adsorbents

4.4 HCl adsorption of Meso-NaY (Leaching) (3 replications)

The results of HCl adsorption of Meso-NaY (Leaching) in three replications are consistent, as shown in Figure 4.13. The adsorption capacities were still high as listed in Table 4.8. It has been characterized with XRD and XRF to confirm each adsorption bed (top, middle and bottom).
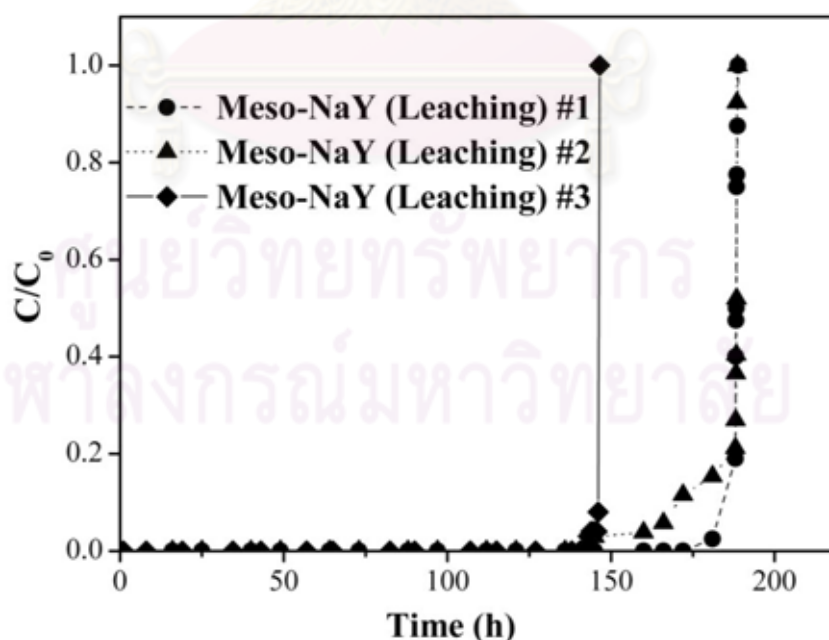

Figure 4.13 HCl breakthrough curves of Meso-NaY (Leaching) in 3 replications.

Table 4.8 Adsorption capacity of HCl of Meso-NaY (Leaching) in 3 replications

Adsorbent	W_{sat} (g_{HCl}/g^*)	W_b (g_{HCl}/g^*)	Bed Capacity
Meso-NaY(Leaching) #1	0.2395	0.2355	0.9984
Meso-NaY(Leaching) #2	0.1849	0.1796	0.9714
Meso-NaY(Leaching) #3	0.1886	0.1805	0.9573
Meso-NaY(Leaching) Average	0.2043	0.1985	0.9757

*g is weight of adsorbents

The XRD patterns of Meso-NaY from each bed (top, middle and bottom) are presented compared with NaCl and Meso-NaY itself, respectively, as shown in Figure 4.14. A sharp and strong peak at 32º and small peak at 46º were observed indicating that NaCl was formed on each adsorption bed. Consequently, the forming of NaCl was occurred by chemisorption reaction between HCl and Na content in Meso-NaY structure. It might be concluded that Na content was high impacted to HCl adsorption.
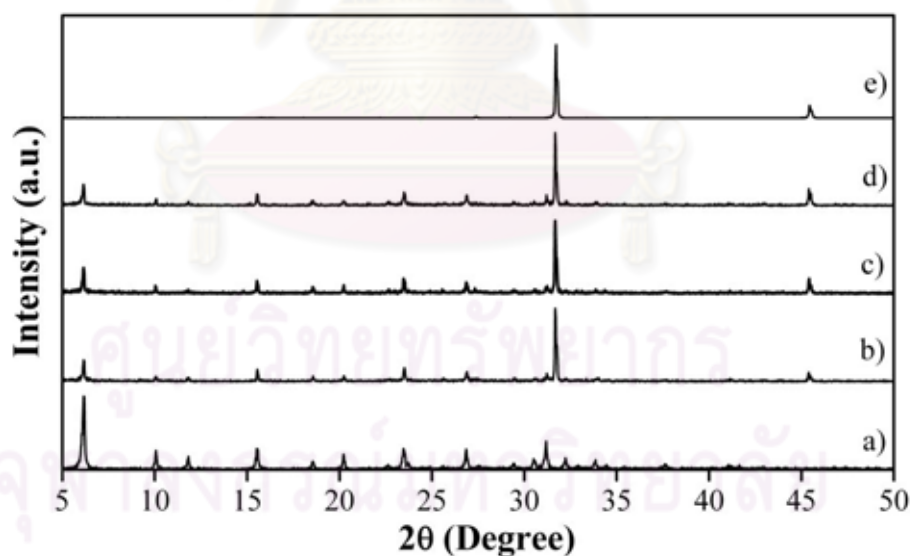

Figure 4.14 XRD patterns of Meso-NaY (Leaching) after HCl adsorption; a) Meso-NaY (Leaching), b) Meso-NaY (Leaching) adsorbed HCl-top, c) Meso-NaY (Leaching) adsorbed HCl-middle, d) Meso-NaY (Leaching) adsorbed HCl-bottom and e) NaCl.

The amount of elements of fresh and spent zeolite NaY and Meso-NaY (Leaching) was investigated the chloride composition as shown in Table 4.9. The chloride content appeared in spent Meso-NaY (Leaching) of 24.34%, 10.38%, and 22.41% in top, middle and bottom, respectively. Elemental balance on Cl should be the key factor to confirm whether the adsorption has been tested correctly. The Na/Cl molar ratio may not balance in each other. This result showed Cl may adsorb not only on Na content but also pore structure.

Table 4.9 Quantity of element in fresh and spent zeolite NaY and Meso-NaY

Samples	Quantity (% by weight)						
	Na_2O	Al_2O_3	SiO_2	Cl	K_2O	CaO	TiO_2
NaY-zeolite	6.64	16.68	53.01	<0.01	0.05	0.36	<0.01
Meso-NaY(Leaching)	5.91	15.74	54.27	<0.01	0.02	<0.01	0.05
- Top	3.75	11.85	36.84	24.34	0.04	0.54	0.05
- Middle	4.50	15.74	52.27	10.58	0.06	5.28	0.04
- Bottom	3.32	12.26	38.45	22.41	0.06	0.44	0.04

4.5 Economic of HCl adsorption study of Meso-NaY (Leaching)

Using of the recipe to synthesize Meso-NaY, the synthesis cost was determined. The calculation was computed under 1 kg of Meso-NaY basic. The purchase cost of the major equipments and chemicals for synthesis of Meso-NaY (Leaching) are summarized in Table 4.10. The synthesis cost with material cost was 7,802.50 Baht/kg in the laboratory scale. Meanwhile, the operating cost was 3,483 Baht/kg of Meso-NaY (Leaching). Thus, the total price of Meso-NaY (Leaching) was 11,286 Baht/kg. Estimated cost of Meso-NaY (Leaching) is higher than commercial cost due to price of laboratory grade chemical, limited equipment and small obtained yield.

Table 4.10 Material cost and wage for the synthesis Meso-NaY (Leaching)

Product	Synthesis cost			Wage Cost		Tatal
	Material	Amount of material	Price (Baht)	Duration (h)	Wage[*]	(Baht)
Na$_2$SiO$_3$ 165.15 g	Rice husk silica	31.38 g	0.5			
	NaOH	16.23 g	1.25			
		Sum	1.75	16	432	433.75
Zeolite NaY 30 g	NaOH	4.21 g	1.25			
	NaAlO2	15.18 g	27.25			
	Oven	24 kW/h	19.50			
	Motor Suction	7 kW/h	21			
	Filter paper	7 paper	14			
	pH tester paper	2 paper	5.4			
		Sum	88.4	19	513	601.4
Meso-NaY (Leaching) 20 g	NaOH	7.2 g	13			
	Motor Suction	8 kW/h	24			
	Heater	0.5 kW/h	1.50			
	Filter paper	6 paper	12			
	pH tester paper	2 paper	5.4			
	Oven	12 kW/h	10			
		Sum	65.9	8	216	281.9
Total for 20 g product			156.1		1,161	1,317
Total for 1 kg product			7803		3,483[**]	11,286

[*]Wage = (Duration for synthesis) x (Minimum wage)

where minimum wage is 27 baht/h (Department of Labor Protection and welfare, 2011).

[**]3,483come from 50 batches (approximately 3 cycles)

1 cycle can synthesize Meso- NaY (Leaching) of 400 g (in 20 batches).

CHAPTER V

CONCLUSIONS AND RECOMMENDATIONS

5.1 Conclusions

The Meso-NaY without magnesium from rice husk silica can be synthesized and evaluated the adsorption capacity of synthesized material for removal of hydrogen chloride. Accordingly to the results, the conclusions could be addressed as follows;

1) Zeolite NaY and Meso-NaY were synthesized from rice husk silica.

2) The structure of Meso-NaY (Leaching) and Meso-NaY (Template) were still remained after mesoporous modification and crystallite size were bigger, compared with original zeolite NaY.

3) The surface area and pore volume of Meso-NaY (Leaching) powder were higher (653 m^2/g, 0.5889 cm^3/g), compared with original zeolite NaY (533 m^2/g, 0.3302 cm^3/g)

4) After addition of positive charge of Mg on Meso-NaY (Leaching), the structure of Mg/Meso-NaY (Leaching) was still remained and the surface area was decreased dramatically (175 m^2/g).

5) The surface area of pelleted Meso-NaY (Leaching) from pressing method was higher than that from extrusion and mechanical coating methods.

6) The spent adsorbent possessed NaCl in its structure, after the HCl removal

7) The addition of positive charge of Mg could not improve the removal performance.

8) The pelleted Meso-NaY (Leaching) from pressing method showed better in HCl adsorption (Wb = 0.1985 g_{HCl}/g) than commercial one (Wb = 0.0819 g_{HCl}/g).

5.2 Recommendations

1) Since the contaminants in natural gas are not only HCl, the synthesized Meso-NaY should be tested on those contaminants such as vinyl chloride monomer (VCM). Moreover, the mixture of both contaminants (HCl and VCM) should be tested simultaneously.

2) Even though the laboratory scale was successful, up-scale removal test in the same residence time should be carried out.

3) Hydrodynamic work should be tested for the empirical for the up-scale operation.

REFERENCES

Abello, S., Bonilla, A., and Pe´rez-Ramı´rez, J. Mesoporous ZSM-5 zeolite catalysts prepared by desilication with organic hydroxides and comparison with NaOH leaching. Journal of Applied Catalysis A: General 364 (2009): 191-198.

Chang, R. Chemistry. 9th edition. McGraw international. (2007).

Chatterjee, A., Ebina, T., Iwasaki, T., and Mizukami, F. Chlorofluorocarbons adsorption structures and energetic over faujasite type zeolites a first principle study. Journal of Molecular Structure (Theochem) 630 (2003): 233-242.

Chumee, J., Grisdanurak, N., Neramittagapon, A., and Wittayakun, J. Catalysts supported on MCM-41 synthesized with rice husk silica and their performance for phenol hydroxylation. Journal of Science Technology Advance Material 10 (2009): 1-6.

Crittenden, B., and Thomas. W.J. Adsorption Technology and Design. 1st edition. Biddles Ltd. (1998).

Department of Labor Protection and welfare, Minimum Wage Commission[Online], Department of Labor Protection and welfare. Available from: http://www.labour.go.th/news/file/minimumWage.pdf [2011, May 10].

Gammon, E. General Chemistry. 9th edition. Houghton Miffin Company, Boston. (2007).

Garcı´a, R.A., Serrano, D.P., and Oteroj, D. Catalytic cracking of HDPE over hybrid zeolitic–mesoporous. Journal of Analytical and Applied Pyrolysis 74 (2005): 379-386.

Grisdanurak, N., and Wittayakun, J. Journal of Catalysis: Fundamental and Application. 1st edition. Thammasat University. (2004).

Hue L., and others Process for removing chlorine-containing compounds from hydrocarbon streams. United States Patent 3,935,295 (1976).

Keller, J., and Sraudt, R. Gas Adsorption Equilibria: Experimental Methods and Adsorptive Isotherms. Sringer Science & Business Medai Inc. (2005).

Kordatos, K., Gavela, S., Ntziouni, A., Pistiolas, K.N., Kyritsi, A., and Kasselouri-Rigopoulou, V. Synthesis of highly siliceous ZSM-5 zeolite using silica from rice husk ash. Journal of Microporous and Mesoporous Materials 115 (2008): 189–196.

Lewis, W.K., and Whitman, W.G. Principles of Gas Absorption. Journal of Industrial and Engineering Chemistry 16 (1924): 1215-1220.

Liu S. Preformed zeolite precursor route for synthesis of mesoporous X zeolite. Journal of Colloids and Surfaces A: Physicochem Eng 318 (2008): 269-274.

McWilliams, and others. Guard bed catalyst for organic chloride removal from hydrocarbon feed. United States Patent 4,721,824 (1988).

Mohamed, M.M., Zidan, F.I., and Thabet, M. Synthesis of ZSM-5 zeolite from rice husk ash: Characterization and implications for photocatalytic degradation catalysts. Journal of Microporous and Mesoporous Materials 108 (2008): 193-203.

Park, S.J., and Jin, S.Y. Effect of nickel Electroplating on HCl removal efficiency of Activated carbon fiber. Journal of Industrial Engineering Chemical 11 (2005): 395-399.

Rahman, M.J., Bozadjiev, P., and Pelovski, Y. Studies on the effects of some additives on the physicomechanical properties of urea-ammonium sulphate (UAS) pellets. Journal of Fertilizer Research 38 (1994): 89-93.

Rahman, M.M., Hasnida, N., and Wan N. Preparation of Zeolite Y Using Local Raw Material Rice Husk as a Silica Source. Journal of Scientific Research 2 (2009): 285-291.

Realpe R.C., and Ramírez, J.P. ZSM-5 zeolites prepared by a two-step route comprising sodium aluminate and acid treatments. Journal of Microporous and Mesoporous Materials 128 (2010): 91-100.

Ruthven, D.M. Principles of Adsorption and Adsorption Process. John Wliley & Sons Inc. (1984).

Sang, S., Liu, Z., Tian, P, Liu Z., Qu L., and Zhang Y. Synthesis of small crystals zeolite NaY Journal of Materials Letters 60 (2006): 1131–1133.

Saporm, Y. Utilization of MCM-41 synthesized from rice husk ash silica as an air sampling material. King Mongut's University of Technology Thonburi. (2005).

Sechrist. Method for reducing chloride emissions from a catalyst regeneration process. United States Patent 5,837,636 (1988).

Twigg, M.V., and Spencer M. S. Deactivation of supported copper metal catalysts for hydrogenation reactions. Journal of Applied Catalysis A: General 212 (2001): 161-174.

Walton, K.S., Abney, M.B., and Levan, M.D. CO_2 adsorption in Y and X zeolites modified by alkali metal cation exchange. Journal of Microporous and Mesoporous Materials 91 (2006): 78-84.

Wittayakun, J., Khemthong, P., and Prayoonpokarach, S. Synthesis and characterization of zeolite NaY from rice husk silica. Journal of Korean Chemistry 25 (2008): 861-864.

Yang, R.T., and Ed. <u>Adsorbents: Fundamentals and Applications.</u> New Jersey, John Wiley and Sons, INC. (2003).

Yoshida, H., Yun, L, Nakayama, H., and Hirohashi, M. Fabrication of TiO_2 film by mechanical coating technique and its photocatalytic activity. <u>Journal of Alloys and Compounds</u> 475 (2009): 383-386.

APPENDICES

APPENDIX A

The calculation of HCl adsorption capacity

The HCl adsorption capacity by equation was calculated by equation A-1 to A-3:

$$W_{sat} = \frac{F_A \times \text{Area above the breakthrough curve graph}}{\text{Mass of adsorbent per unit cross section area of bed}} \quad \ldots\ldots\ldots\ldots(A-1)$$

$$W_b = \frac{F_A \times \text{Area above the breakthrough curve graph at breakpoint}}{\text{Mass of adsorbent per unit cross section area of bed}} \quad \ldots.(A-2)$$

$$\text{Bed capacity} = \frac{W_b}{W_{sat}} \quad \ldots\ldots\ldots\ldots\ldots\ldots\ldots\ldots.(A-3)$$
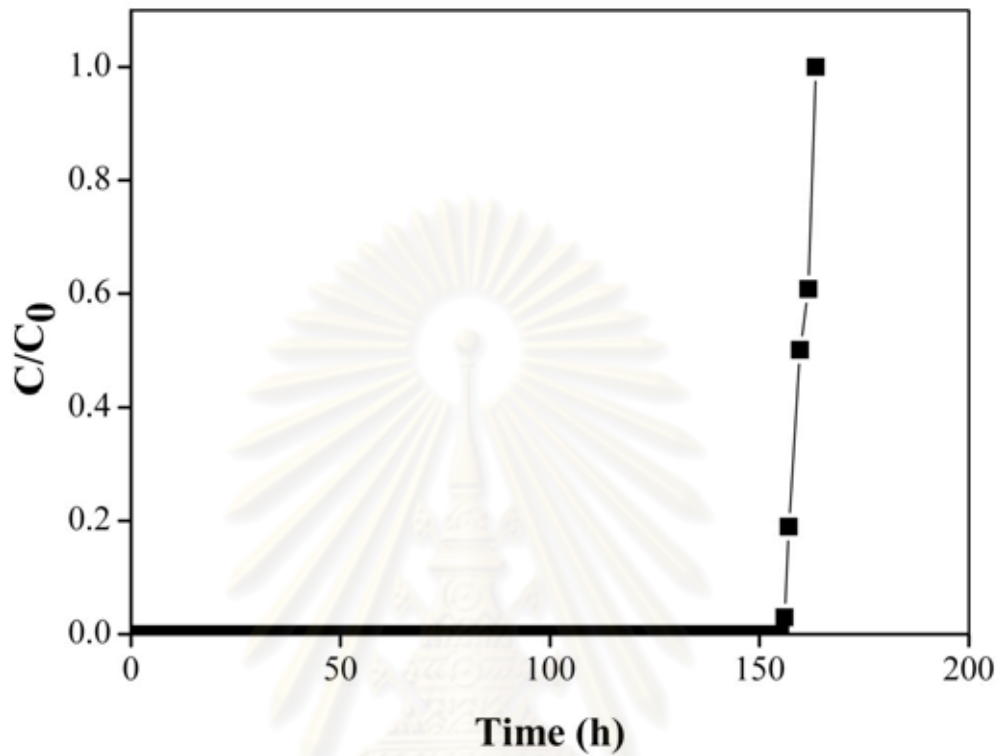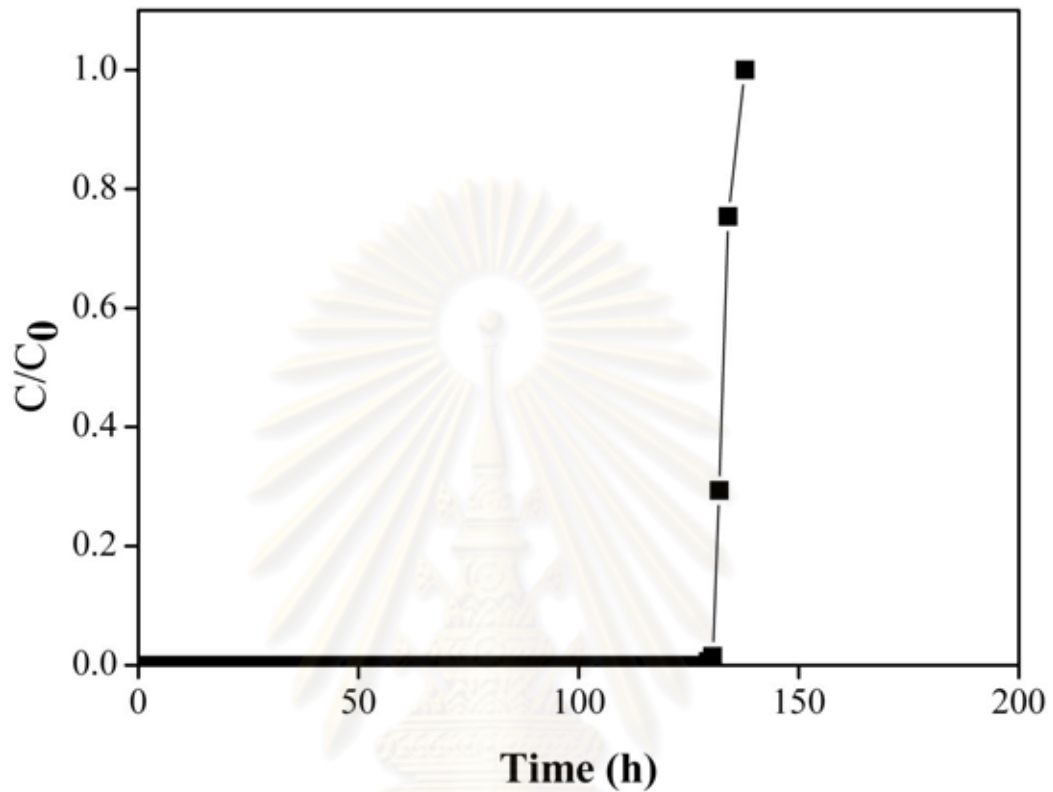
1. Commercial

Figure A-1 HCl breakthrough curves on commercial.

F_A = Solute feed rate (g/cm^{2}h)

F_A = $u_0 c_0 M$

u_0 = Velocity of solute (cm/s)

c_0 = Concentration (mol/cm^3)

M = Molecular weight (g/mol)

$$F_A = \left(\frac{50 \ \frac{cm^3}{min}}{\frac{\pi(1)^2}{4} \ cm^2} \right) \left(\frac{500 \times 10^{-6}}{22,400} \times \frac{273}{301} \times \frac{760}{760} \right) \frac{mol}{cm^3} \ 36.5 \ \frac{g}{mol}$$

$$F_A = 4.7 \times 10^{-5} \frac{g}{cm^2\ min} \quad 2.82 \times 10^{-3} \frac{g}{cm^2\ h}$$

$$\text{Area above the graph} = \int_0^{163.5} (1 - \frac{c}{c_0}\ dt)$$
$$= 159.91\ h$$

$$\text{Mass of asorbent per unit cross sectional area of bed} = 6 \times 0.9184 \frac{g}{cm^2}$$
$$= 5.5104 \frac{g}{cm^2}$$

$$W_{sat} = \frac{2.82 \times 10^{-3} \frac{g}{cm^2 h} \times 159.5\ h}{5.4104 \frac{g}{cm^2 h}} = 0.0813 \frac{g\ HCl}{g\ adsorbent}$$

Break point condition; C/Co = 0.05

$$\text{Area above the graph} = \int_0^{156} (1 - \frac{c}{c_0}\ dt)$$
$$= 155.98\ h$$

$$W_b = \frac{2.82 \times 10^{-3} \frac{g}{cm^2 h} \times 155.98\ h}{5.4104 \frac{g}{cm^2 h}} = 0.0793 \frac{g\ HCl}{g\ adsorbent}$$

$$\text{Bed capacity} = \frac{0.0793 \frac{g_{HCl}}{g_{adsorbent}}}{0.0813 \frac{g_{HCl}}{g_{adsorbent}}} = 0.9754$$

2. Zeolite NaY

Figure A-2 HCl breakthrough curves on zeolite NaY #1.

F_A = Solute feed rate (g/cm^{2}h)

$F_A = u_0 c_0 M$

u_0 = Velocity of solute (cm/s)

c_0 = Concentration (mol/cm^3)

M = Molecular weight (g/mol)

$$F_A = \left(\frac{50 \ \frac{cm^3}{min}}{\frac{\pi(1)^2}{4} \ cm^2} \right) \left(\frac{500 \times 10^{-6}}{22,400} \times \frac{273}{301} \times \frac{760}{760} \right) \frac{mol}{cm^3} \ 36.5 \ \frac{g}{mol}$$

$$F_A = 4.7 \times 10^{-5} \frac{g}{cm^2 \, min} \quad 2.82 \times 10^{-3} \frac{g}{cm^2 \, h}$$

$$\text{Area above the graph} = \int_0^{137.83} (1 - \frac{c}{c_0} \, dt)$$
$$= 133.18 \, h$$

$$\text{Mass of asorbent per unit cross sectional area of bed} = 6 \times 0.5940 \frac{g}{cm^2}$$
$$= 3.5640 \quad \frac{g}{cm^2}$$

$$W_{sat} = \frac{2.82 \times 10^{-3} \frac{g}{cm^2 h} \times 133.18 \, h}{3.5640 \frac{g}{cm^2 h}} = 0.1047 \frac{g_{HCl}}{g_{adsorbent}}$$

Break point condition; C/Co = 0.05

$$\text{Area above the graph} = \int_0^{130.5} (1 - \frac{c}{c_0} \, dt)$$
$$= 132.99 \, h$$

$$W_b = \frac{2.82 \times 10^{-3} \frac{g}{cm^2 h} \times 132.99 \, h}{3.5640 \frac{g}{cm^2 h}} = 0.1046 \frac{g_{HCl}}{g_{adsorbent}}$$

$$\text{Bed capacity} = \frac{0.1046 \frac{g_{HCl}}{g_{adsorbent}}}{0.1047 \frac{g_{HCl}}{g_{adsorbent}}} = 0.9982$$
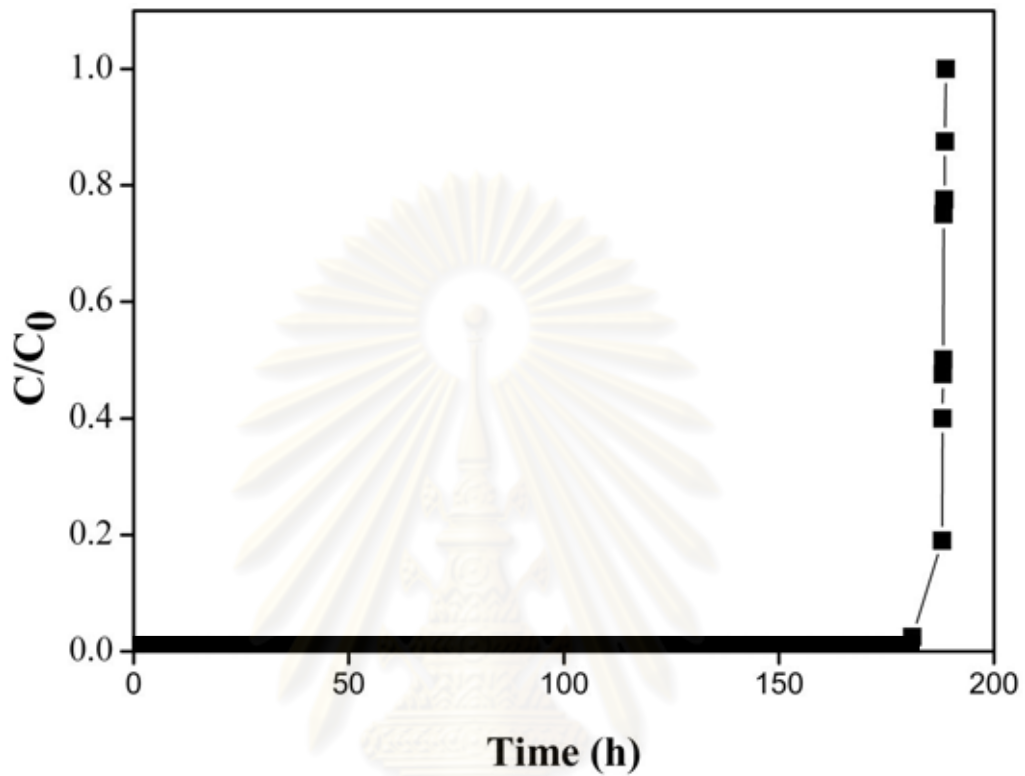
3. Meso-NaY (PDADMAC)

Figure A-3 HCl breakthrough curves on Meso-NaY (PDADAMAC).

F_A = Solute feed rate (g/cm^{2}h)

$F_A = u_0 c_0 M$

u_0 = Velocity of solute (cm/s)

c_0 = Concentration (mol/cm^3)

M = Molecular weight (g/mol)

$$F_A = \left(\frac{50 \ \frac{cm^3}{min}}{\frac{\pi(1)^2}{4} \ cm^2} \right) \left(\frac{500 \times 10^{-6}}{22{,}400} \times \frac{273}{301} \times \frac{760}{760} \right) \frac{mol}{cm^3} \ 36.5 \ \frac{g}{mol}$$

$$F_A = 4.7 \times 10^{-5} \; \frac{g}{cm^2 \; min} \quad 2.82 \times 10^{-3} \; \frac{g}{cm^2 \; h}$$

$$\text{Area above the graph} = \int_0^{137} (1 - \frac{c}{c_0} \; dt)$$
$$= 130.5 \; h$$

$$\text{Mass of asorbent per unit cross sectional area of bed} = 6 \times 0.5700 \; \frac{g}{cm^2}$$
$$= 3.42 \quad \frac{g}{cm^2}$$

$$W_{sat} = \frac{2.82 \times 10^{-3} \; \frac{g}{cm^2 h} \times 130.5 \; h}{3.42 \; \frac{g}{cm^2 h}} = 0.1076 \; \frac{g \; _{HCl}}{g \; _{adsorbent}}$$

Break point condition; C/Co = 0.05

$$\text{Area above the graph} = \int_0^{131.25} (1 - \frac{c}{c_0} \; dt)$$
$$= 124.55 \; h$$

$$W_b = \frac{2.82 \times 10^{-3} \; \frac{g}{cm^2 h} \times 124.55 \; h}{3.42 \; \frac{g}{cm^2 h}} = 0.1027 \; \frac{g \; _{HCl}}{g \; _{adsorbent}}$$

$$\text{Bed capacity} = \frac{0.1027 \; \frac{g_{HCl}}{g_{adsorbent}}}{0.1076 \; \frac{g_{HCl}}{g_{adsorbent}}} = 0.9545$$
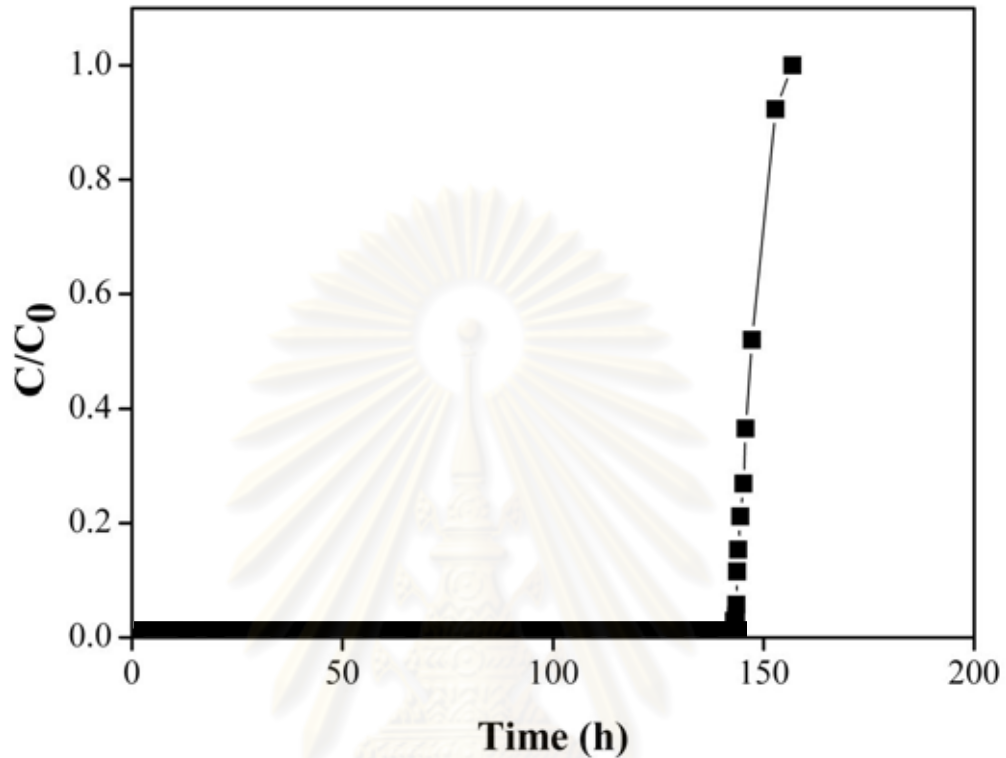
4. Meso-NaY(Leaching) (pressing) #1

Figure A-4 HCl breakthrough curves on Meso-NaY (Leaching) (pressing) #1.

F_A = Solute feed rate (g/cm^{2}h)

$F_A = u_0c_0M$

u_0 = Velocity of solute (cm/s)

c_0 = Concentration (mol/cm^3)

M = Molecular weight (g/mol)

$$F_A = \left(\frac{50 \ \frac{cm^3}{min}}{\frac{\pi(1)^2}{4} \ cm^2} \right) \left(\frac{500 \times 10^{-6}}{22,400} \times \frac{273}{301} \times \frac{760}{760} \right) \frac{mol}{cm^3} \ 36.5 \ \frac{g}{mol}$$

$$F_A = 4.7 \times 10^{-5} \ \frac{g}{cm^2 \ min} \quad 2.82 \times 10^{-3} \ \frac{g}{cm^2 \ h}$$

$$\text{Area above the graph} = \int_{0}^{200.503} \left(1 - \frac{c}{c_0} \ dt\right)$$
$$= 188.46 \ h$$

$$\text{Mass of asorbent per unit cross sectional area of bed} = 6 \times 0.3732 \ \frac{g}{cm^2}$$
$$= 2.2392 \ \frac{g}{cm^2}$$

$$W_{sat} = \frac{2.82 \times 10^{-3} \ \frac{g}{cm^2 h} \times 188.46 \ h}{2.2392 \ \frac{g}{cm^2 h}} = 0.2359 \ \frac{g \ HCl}{g \ adsorbent}$$

Break point condition; C/Co = 0.05

$$\text{Area above the graph} = \int_{0}^{188} \left(1 - \frac{c}{c_0} \ dt\right)$$
$$= 188.15 \ h$$

$$W_b = \frac{2.82 \times 10^{-3} \ \frac{g}{cm^2 h} \times 188.15 \ h}{2.2392 \ \frac{g}{cm^2 h}} = 0.2355 \ \frac{g \ HCl}{g \ adsorbent}$$

$$\text{Bed capacity} = \frac{0.2355 \ \frac{g_{HCl}}{g_{adsorbent}}}{0.2359 \ \frac{g_{HCl}}{g_{adsorbent}}} = 0.9983$$

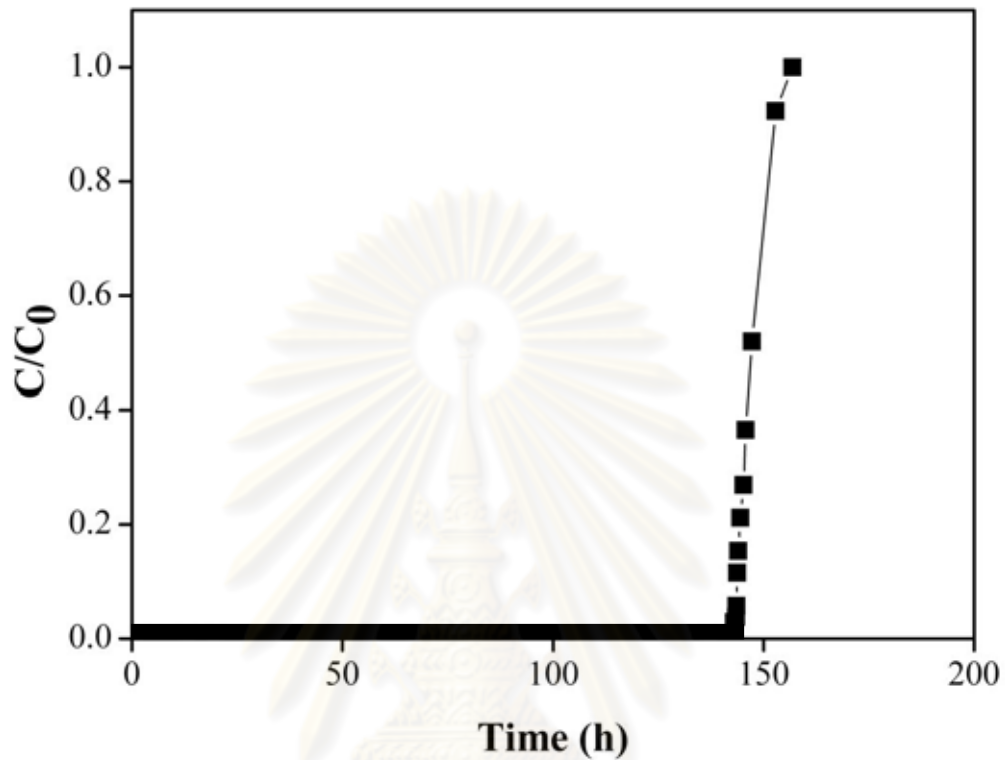## 5. Meso-NaY (Leaching) (pressing) #2

Figure A-5 HCl breakthrough curves on Meso-NaY (Leaching) (pressing) #2.

F_A = Solute feed rate (g/cm^{2}h)

$F_A = u_0 c_0 M$

u_0 = Velocity of solute (cm/s)

c_0 = Concentration (mol/cm^3)

M = Molecular weight (g/mol)

$$F_A = \left(\frac{50 \ \frac{cm^3}{min}}{\frac{\pi(1)^2}{4} \ cm^2} \right) \left(\frac{500 \times 10^{-6}}{22,400} \times \frac{273}{301} \times \frac{760}{760} \right) \frac{mol}{cm^3} \ 36.5 \ \frac{g}{mol}$$

$$F_A = 4.7 \times 10^{-5} \; \frac{g}{cm^2 \, min} \quad 2.82 \times 10^{-3} \; \frac{g}{cm^2 \, h}$$

$$\text{Area above the graph} = \int_0^{156.85} (1 - \frac{c}{c_0} \, dt)$$
$$= 147.72 \; h$$

$$\text{Mass of asorbent per unit cross sectional area of bed} = 6 \times 0.3732 \; \frac{g}{cm^2}$$
$$= 2.2392 \; \frac{g}{cm^2}$$

$$W_{sat} = \frac{2.82 \times 10^{-3} \; \frac{g}{cm^2 h} \times 147.72 \; h}{2.2392 \; \frac{g}{cm^2 h}} = 0.1849 \; \frac{g \; HCl}{g \; adsorbent}$$

Break point condition; C/Co = 0.05

$$\text{Area above the graph} = \int_0^{149.6} (1 - \frac{c}{c_0} \, dt)$$
$$= 143.49 \; h$$

$$W_b = \frac{2.82 \times 10^{-3} \; \frac{g}{cm^2 h} \times 143.49 \; h}{2.2392 \; \frac{g}{cm^2 h}} = 0.1796 \; \frac{g \; HCl}{g \; adsorbent}$$

$$\text{Bed capacity} = \frac{0.1796 \; \frac{g_{HCl}}{g_{adsorbent}}}{0.1849 \; \frac{g_{HCl}}{g_{adsorbent}}} = 0.9714$$
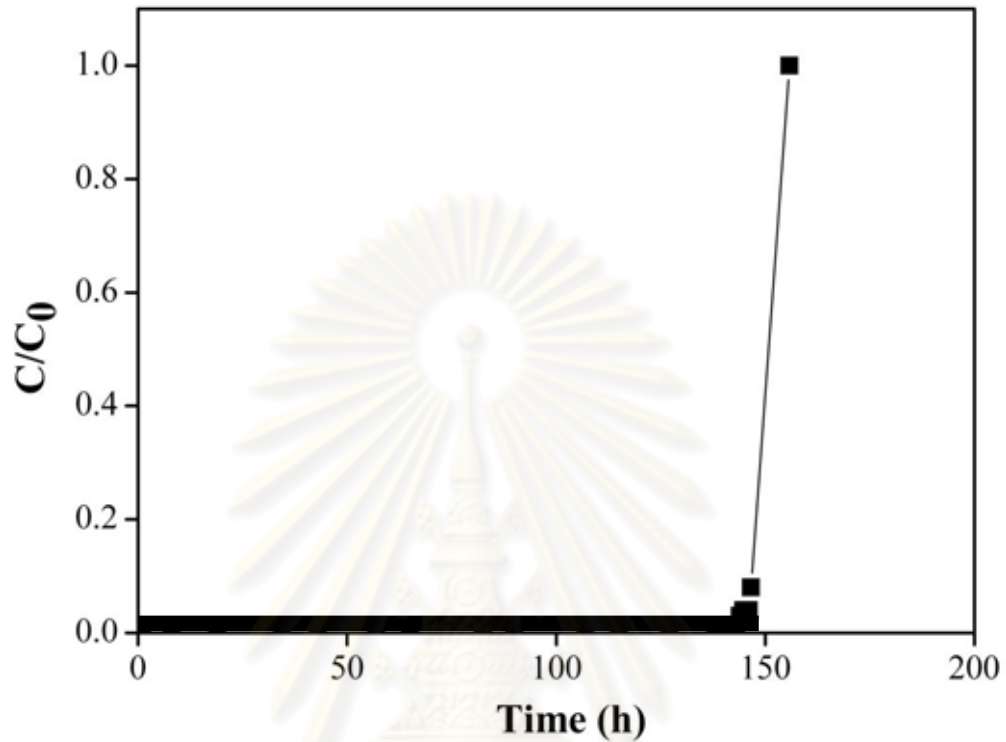
6. Meso-NaY (Leaching) (pressing) #3

Figure A-6 HCl breakthrough curves on Meso-NaY (Leaching) (pressing) #3.

F_A = Solute feed rate (g/cm^{2}h)

F_A = $u_0 c_0 M$

u_0 = Velocity of solute (cm/s)

c_0 = Concentration (mol/cm^3)

M = Molecular weight (g/mol)

$$F_A = \left(\frac{50 \ \frac{cm^3}{min}}{\frac{\pi(1)^2}{4} \ cm^2} \right) \left(\frac{500 \times 10^{-6}}{22,400} \times \frac{273}{301} \times \frac{760}{760} \right) \frac{mol}{cm^3} \ 36.5 \ \frac{g}{mol}$$

$$F_A = 4.7 \times 10^{-5} \ \frac{g}{cm^2 \ min} \quad 2.82 \times 10^{-3} \ \frac{g}{cm^2 \ h}$$

Area above the graph $= \int_{0}^{155.82} (1- \frac{c}{c_0} \ dt)$

$= 150.69$ h

Mass of asorbent per unit cross sectional area of bed $= 6 \times 0.3732 \ \frac{g}{cm^2}$

$= 2.2392 \ \frac{g}{cm^2}$

$$W_{sat} = \frac{2.82 \times 10^{-3} \ \frac{g}{cm^2 h} \times 150.69 \ h}{2.2392 \ \frac{g}{cm^2 h}} = 0.1886 \ \frac{g \ HCl}{g \ adsorbent}$$

Break point condition; C/Co = 0.05

Area above the graph $= \int_{0}^{148.25} (1- \frac{c}{c_0} \ dt)$

$= 144.25$ h

$$W_b = \frac{2.82 \times 10^{-3} \ \frac{g}{cm^2 h} \times 144.25 \ h}{2.2392 \ \frac{g}{cm^2 h}} = 0.1805 \ \frac{g \ HCl}{g \ adsorbent}$$

Bed capacity $= \dfrac{0.1805 \ \frac{g_{HCl}}{g_{adsorbent}}}{0.1886 \ \frac{g_{HCl}}{g_{adsorbent}}} = 0.9571$

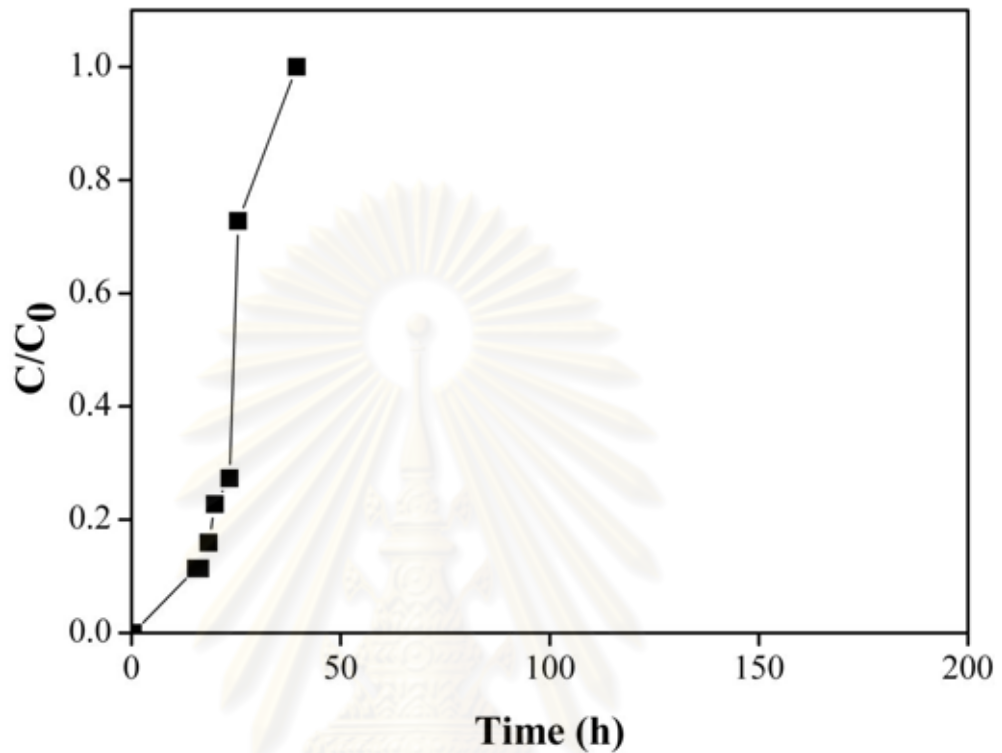## 7. Mg/Meso-NaY (PDADMAC)

Figure A-7 HCl breakthrough curves on Mg/Meso-NaY (PDADMAC).

F_A = Solute feed rate (g/cm^{2}h)

$F_A = u_0 c_0 M$

u_0 = Velocity of solute (cm/s)

c_0 = Concentration (mol/cm^3)

M = Molecular weight (g/mol)

$$F_A = \left(\frac{50 \frac{cm^3}{min}}{\frac{\pi(1)^2}{4} cm^2} \right) \left(\frac{500 \times 10^{-6}}{22,400} \times \frac{273}{301} \times \frac{760}{760} \right) \frac{mol}{cm^3} \; 36.5 \; \frac{g}{mol}$$

$$F_A = 4.7 \times 10^{-5} \ \frac{g}{cm^2 \ min} \quad 2.82 \times 10^{-3} \ \frac{g}{cm^2 \ h}$$

$$\text{Area above the graph} = \int_{0}^{39.5} (1 - \frac{c}{c_0} \ dt)$$
$$= 37.5 \ h$$

$$\text{Mass of asorbent per unit cross sectional area of bed} = 6 \times 0.6298 \ \frac{g}{cm^2}$$
$$= 37.5 \ \frac{g}{cm^2}$$

$$W_{sat} = \frac{2.82 \times 10^{-3} \ \frac{g}{cm^2 h} \ \times 37.5 \ h}{3.7788 \ \frac{g}{cm^2 h}} = 0.0178 \ \frac{g \ HCl}{g \ adsorbent}$$

Break point condition; C/Co = 0.05

$$\text{Area above the graph} = \int_{0}^{35.755} (1 - \frac{c}{c_0} \ dt)$$
$$= 5.83 \ h$$

$$W_b = \frac{2.82 \times 10^{-3} \ \frac{g}{cm^2 h} \ \times 5.85 \ h}{3.7788 \ \frac{g}{cm^2 h}} = 0.0043 \ \frac{g \ HCl}{g \ adsorbent}$$

$$\text{Bed capacity} = \frac{0.0043 \ \frac{g_{HCl}}{g_{adsorbent}}}{0.0178 \ \frac{g_{HCl}}{g_{adsorbent}}} = 0.2416$$
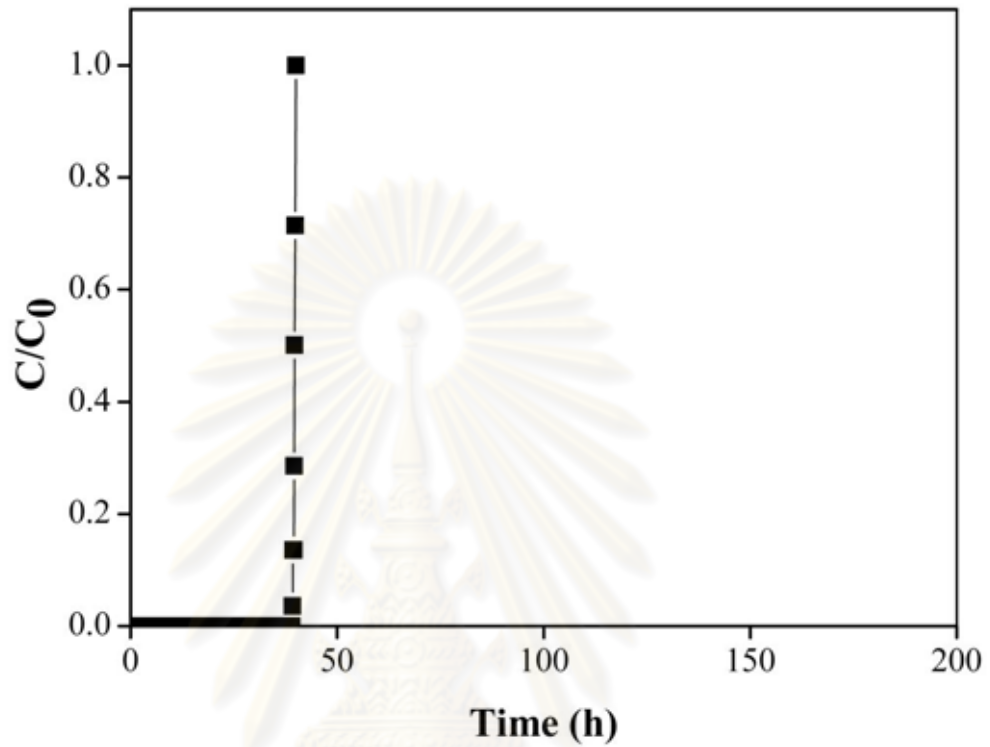
8. Mg/Meso-NaY (Leaching)

Figure A-8 HCl breakthrough curves on Mg/Meso-NaY (Leaching).

F_A = Solute feed rate (g/cm^{2}h)

F_A = u_0c_0M

u_0 = Velocity of solute (cm/s)

c_0 = Concentration (mol/cm^3)

M = Molecular weight (g/mol)

$$F_A = \left(\dfrac{50 \ \frac{cm^3}{min}}{\frac{\pi(1)^2}{4} \ cm^2} \right) \left(\dfrac{500 \times 10^{-6}}{22,400} \times \dfrac{273}{301} \times \dfrac{760}{760} \right) \dfrac{mol}{cm^3} \ 36.5 \ \dfrac{g}{mol}$$

$$F_A = 4.7 \times 10^{-5} \frac{g}{cm^2 \, min} \quad 2.82 \times 10^{-3} \frac{g}{cm^2 \, h}$$

$$\text{Area above the graph} = \int_0^{40} (1 - \frac{c}{c_0} \, dt)$$
$$= 39.67 \, h$$

$$\text{Mass of asorbent per unit cross sectional area of bed} = 6 \times 0.4 \frac{g}{cm^2}$$
$$= 2.4 \frac{g}{cm^2}$$

$$W_{sat} = \frac{2.82 \times 10^{-3} \frac{g}{cm^2 h} \times 39.67 \, h}{2.4 \frac{g}{cm^2 h}} = 0.0463 \frac{g_{HCl}}{g_{adsorbent}}$$

<u>Break point condition; C/Co = 0.05</u>

$$\text{Area above the graph} = \int_0^{39.04} (1 - \frac{c}{c_0} \, dt)$$
$$= 39.65 \, h$$

$$W_b = \frac{2.82 \times 10^{-3} \frac{g}{cm^2 h} \times 39.65 \, h}{2.4 \frac{g}{cm^2 h}} = 0.0463 \frac{g_{HCl}}{g_{adsorbent}}$$

$$\text{Bed capacity} = \frac{0.0463 \frac{g_{HCl}}{g_{adsorbent}}}{0.0463 \frac{g_{HCl}}{g_{adsorbent}}} = 0.9995$$
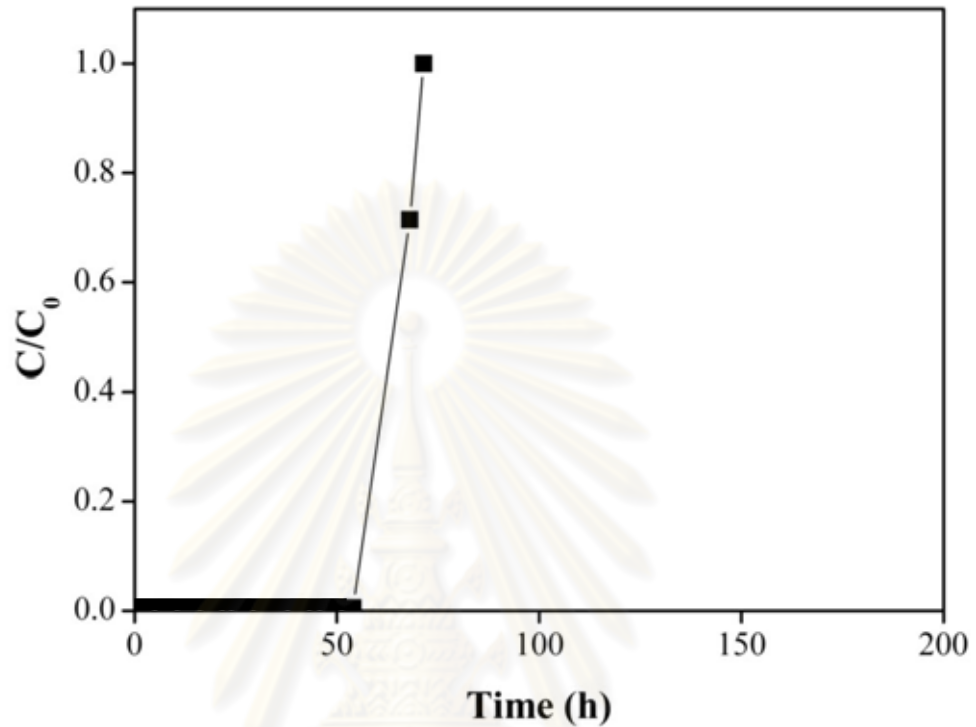
9. Alumina ball

Figure A-9 HCl breakthrough curves on Allumina ball.

F_A = Solute feed rate (g/cm²h)

$F_A = u_0 c_0 M$

u_0 = Velocity of solute (cm/s)

c_0 = Concentration (mol/cm³)

M = Molecular weight (g/mol)

$$F_A = \left(\frac{50 \frac{cm^3}{min}}{\frac{\pi(1)^2}{4} cm^2} \right) \left(\frac{500 \times 10^{-6}}{22,400} \times \frac{273}{301} \times \frac{760}{760} \right) \frac{mol}{cm^3} \ 36.5 \frac{g}{mol}$$

$$F_A = 4.7 \times 10^{-5} \; \frac{g}{cm^2 \, min} \quad 2.82 \times 10^{-3} \; \frac{g}{cm^2 \, h}$$

$$\text{Area above the graph} = \int_0^{71.5} (1 - \frac{c}{c_0} \, dt)$$
$$= 71.5 \text{ h}$$

$$\text{Mass of asorbent per unit cross sectional area of bed} = 6 \times 0.5496 \; \frac{g}{cm^2}$$
$$= 3.30 \; \frac{g}{cm^2}$$

$$W_{sat} = \frac{2.82 \times 10^{-3} \; \frac{g}{cm^2 h} \times 71.50 \text{ h}}{3.30 \; \frac{g}{cm^2 h}} = 0.0608 \; \frac{g \, HCl}{g \, adsorbent}$$

Break point condition; C/Co = 0.05

$$\text{Area above the graph} = \int_0^{66} (1 - \frac{c}{c_0} \, dt)$$
$$= 52.95 \text{ h}$$

$$W_b = \frac{2.82 \times 10^{-3} \; \frac{g}{cm^2 h} \times 52.95 \text{ h}}{3.30 \; \frac{g}{cm^2 h}} = 0.0450 \; \frac{g \, HCl}{g \, adsorbent}$$

$$\text{Bed capacity} = \frac{0.0450 \; \frac{g_{HCl}}{g_{adsorbent}}}{0.0608 \; \frac{g_{HCl}}{g_{adsorbent}}} = 0.7046$$

10.Bentonite clay

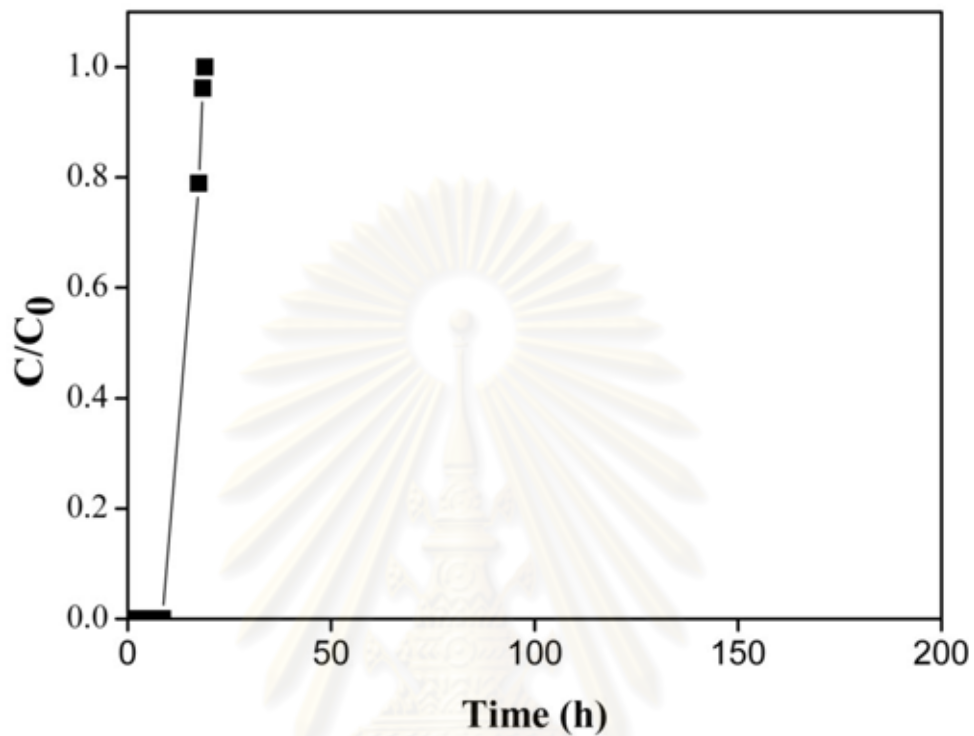**Figure A-10** HCl breakthrough curves on Bentonite clay.

F_A = Solute feed rate (g/cm^{2}h)

F_A = u_0c_0M

u_0 = Velocity of solute (cm/s)

c_0 = Concentration (mol/cm^3)

M = Molecular weight (g/mol)

$$F_A = \left(\frac{50 \ \frac{cm^3}{min}}{\frac{\pi(1)^2}{4} \ cm^2} \right) \left(\frac{500 \times 10^{-6}}{22,400} \times \frac{273}{301} \times \frac{760}{760} \right) \frac{mol}{cm^3} \ 36.5 \ \frac{g}{mol}$$

$$F_A = 4.7 \times 10^{-5} \frac{g}{cm^2 \, min} \quad 2.82 \times 10^{-3} \frac{g}{cm^2 \, h}$$

$$\text{Area above the graph} = \int_0^{19} (1 - \frac{c}{c_0} \, dt)$$
$$= 14.09 \, h$$

$$\text{Mass of asorbent per unit cross sectional area of bed} = 6 \times 0.9285 \frac{g}{cm^2}$$
$$= 5.571 \frac{g}{cm^2}$$

$$W_{sat} = \frac{2.82 \times 10^{-3} \frac{g}{cm^2 h} \times 14.09 \, h}{5.571 \frac{g}{cm^2 h}} = 0.0071 \frac{g_{HCl}}{g_{adsorbent}}$$

Break point condition; C/Co = 0.05

$$\text{Area above the graph} = \int_0^{8.5} (1 - \frac{c}{c_0} \, dt)$$
$$= 9.23 \, h$$

$$W_b = \frac{2.82 \times 10^{-3} \frac{g}{cm^2 h} \times 9.23 \, h}{5.571 \frac{g}{cm^2 h}} = 0.0046 \frac{g_{HCl}}{g_{adsorbent}}$$

$$\text{Bed capacity} = \frac{0.0046 \frac{g_{HCl}}{g_{adsorbent}}}{0.0071 \frac{g_{HCl}}{g_{adsorbent}}} = 0.6551$$

11.Meso-NaY (Leaching) (Meachanical coating)

Figure A-11 HCl breakthrough curves on Meso-NaY (Leaching)
(Meachanical coating).

F_A = Solute feed rate (g/cm^{2}h)

$F_A = u_0 c_0 M$

u_0 = Velocity of solute (cm/s)

c_0 = Concentration (mol/cm^3)

M = Molecular weight (g/mol)

$$F_A = \left(\frac{50 \ \frac{cm^3}{min}}{\frac{\pi(1)^2}{4} \ cm^2} \right) \left(\frac{500 \times 10^{-6}}{22,400} \times \frac{273}{301} \times \frac{760}{760} \right) \frac{mol}{cm^3} \ 36.5 \ \frac{g}{mol}$$

F_A = 4.7 x 10^{-5} _____ g   2.82 x 10^{-3} ____ g

$$\overline{\text{cm}^2 \text{ min}} \qquad\qquad \overline{\text{cm}^2 \text{ h}}$$

Area above the graph $= \displaystyle\int_{0}^{66.55} (1- \frac{c}{c_0} \, dt)$

$= 64.11 \text{ h}$

Mass of asorbent per unit cross sectional area of bed $= 6 \times 0.4035 \, \dfrac{g}{cm^2}$

$= 2.421 \quad \dfrac{g}{cm^2}$

$$W_{sat} = \frac{2.82 \times 10^{-3} \, \dfrac{g}{cm^2 h} \times 64.11 \text{ h}}{2.421 \, \dfrac{g}{cm^2 h}} = 0.0742 \, \dfrac{g_{HCl}}{g_{\text{ adsorbent}}}$$

Break point condition; C/Co = 0.05

Area above the graph $= \displaystyle\int_{0}^{55.50} (1- \frac{c}{c_0} \, dt)$

$= 5.48 \text{ h}$

$$W_{b} = \frac{2.82 \times 10^{-3} \, \dfrac{g}{cm^2 h} \times 5.48 \text{ h}}{2.421 \, \dfrac{g}{cm^2 h}} = 0.0635 \, \dfrac{g_{HCl}}{g_{\text{ adsorbent}}}$$

Bed capacity $= \dfrac{0.0635 \, \dfrac{g_{HCl}}{g_{adsorbent}}}{0.0742 \, \dfrac{g_{HCl}}{g_{adsorbent}}} = 0.9133$

Table A-1 HCl Adsorption efficiency of Meso-NaY (Leaching) (Mechanical coating)

HCl Adsorption efficiency	$g_{HCl}/g_{\text{ adsorbent}}$	$g_{HCl}/{}^{*}g_{adsorbent}$
W_{sat}	0.0742	0.1855
W_{b}	0.0635	0.1587

$*g_{\text{ adsorbent}}$ = Ratio of Meso-NaY (Leaching)/Alumina ball = 4/6
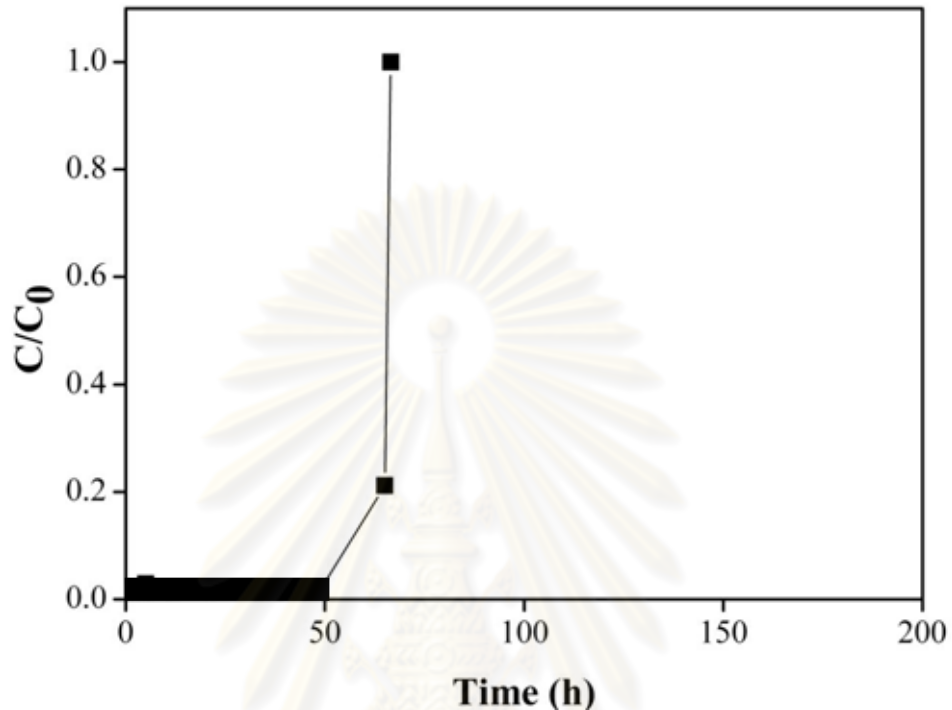
12.Meso-NaY (Leaching) (Extrusion)
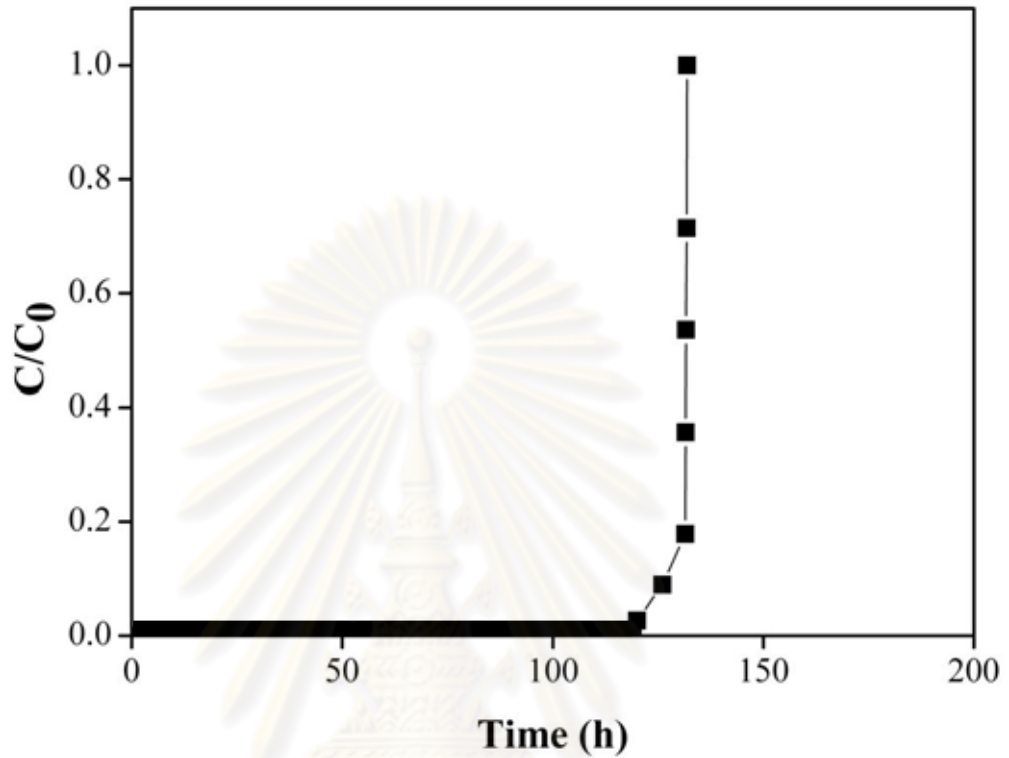
Figure A-12 HCl breakthrough curves on Meso-NaY (Leaching) (Extrusion).

F_A = Solute feed rate (g/cm^{2}h)

$F_A = u_0 c_0 M$

u_0 = Velocity of solute (cm/s)

c_0 = Concentration (mol/cm^3)

M = Molecular weight (g/mol)

$$F_A = \left(\frac{50\ \frac{cm^3}{min}}{\frac{\pi(1)^2}{4}\ cm^2} \right) \left(\frac{500 \times 10^{-6}}{22,400} \times \frac{273}{301} \times \frac{760}{760} \right) \frac{mol}{cm^3}\ 36.5\ \frac{g}{mol}$$

$$F_A = \quad 4.7 \times 10^{-5} \; \frac{g}{cm^2 \; min} \quad 2.82 \times 10^{-3} \; \frac{g}{cm^2 \; h}$$

$$\text{Area above the graph} = \int_{0}^{131.92} (1 - \frac{c}{c_0} \; dt)$$
$$= 130.85 \; h$$

$$\text{Mass of asorbent per unit cross sectional area of bed} = \quad 6 \times 0.6288 \; \frac{g}{cm^2}$$
$$= \quad 3.7728 \quad \frac{g}{cm^2}$$

$$W_{sat} = \frac{2.82 \times 10^{-3} \; \frac{g}{cm^2 h} \times 130.58 \; h}{3.7728 \; \frac{g}{cm^2 h}} = 0.0970 \; \frac{g \; HCl}{g \; adsorbent}$$

Break point condition; C/Co = 0.05

$$\text{Area above the graph} = \int_{0}^{122} (1 - \frac{c}{c_0} \; dt)$$
$$= 121.92 \; h$$

$$W_b = \frac{2.82 \times 10^{-3} \; \frac{g}{cm^2 h} \times 121.92 \; h}{3.7728 \; \frac{g}{cm^2 h}} = 0.0906 \; \frac{g \; HCl}{g \; adsorbent}$$

$$\text{Bed capacity} = \frac{0.0906 \; \frac{g_{HCl}}{g_{adsorbent}}}{0.0970 \; \frac{g_{HCl}}{g_{adsorbent}}} = 0.9309$$

Table A-2 HCl Adsorption efficiency of Meso-NaY (Leaching) (Extrusion)

HCl Adsorption efficiency	g $_{HCl}$/g $_{adsorbent}$	g $_{HCl}$/*g$_{adsorbent}$
W_{sat}	0.0970	0.1212
W_b	0.0906	0.1132

*g $_{adsorbent}$ = Ratio of Meso-NaY (Leaching)/Bentonite clay = 8/2

Table A-3 Adsorption capacity of all synthesized adsorbents

Adsorbent	W_{sat} (g $_{HCl}$/g $_{absorbent}$)	W_b (g $_{HCl}$/g $_{absorbent}$)	Bed capacity
Commercial	0.0813	0.0793	0.9754
Zeolte NaY	0.1047	0.1046	0.9986
Meso-NaY (PDADMAC)	0.1076	0.1027	0.9545
Meso-NaY (Leaching) (Pressing) #1	0.2359	0.2355	0.9984
Meso-NaY (Leaching) (Pressing) #2	0.1849	0.1796	0.9714
Meso-NaY (Leaching) (Pressing) #3	0.1805	0.1886	0.9571
Mg/Meso-NaY (PDADMAC)	0.0178	0.0043	0.2439
Mg/Meso-NaY (Leaching)	0.0463	0.0463	0.9995
Alumina ball	0.0608	0.0405	0.7406
Bentonite clay	0.0071	0.0046	0.6551
Meso-NaY (Leaching) (Mechanical coating)	0.1855	0.1587	0.9133
Meso-NaY (Leaching) (Extrusion)	0.1212	0.1132	0.9309

APPENDIX B

The calculation of crystallite size

The mean crystallite sizes of samples were evaluated by the Scherer equation (B-1):

$$D = \frac{k\lambda}{\beta\cos\theta} \qquad \text{...............................(B-1)}$$

Where λ is 1.54 corresponding to irradiation wavelength, k is 0.9, β is the full width at half maximum of strongest line and θ is the Bragg angle of the most intense peak at a specific phase.

1. Zeolite NaY

$\beta = 6.26 - 6.08 = 0.18$

$\theta = \dfrac{6.2}{2} = 3.1$

$D = \dfrac{(0.90)\,(0.15418)}{0.18\cos3.1} = 0.7720$

2. Standard zeolite NaY

$\beta = 6.24 - 6.12 = 0.12$

$\theta = \dfrac{6.16}{2} = 3.08$

$$D = \frac{(0.90)\,(0.15418)}{0.12\cos3.8} = 1.1547$$

3. Meso-NaY (CTAB)

$\beta = 6.25 - 6.16 = 0.09$

$$\theta = \frac{6.22}{2} = 3.11$$

$$D = \frac{(0.90)\,(0.15418)}{0.09\cos3.11} = 1.5440$$

4. Meso-NaY (PDADMAC)

$\beta = 6.18 - 6.06 = 0.12$

$$\theta = \frac{6.14}{2} = 3.07$$

$$D = \frac{(0.90)\,(0.15418)}{0.12\cos3.1} = 1.1580$$

5. Meso-NaY (Leaching)

$\beta = 6.24 - 6.08 = 0.16$

$$\theta = \frac{6.16}{2} = 3.08$$

$$D = \frac{(0.90)\,(0.15418)}{0.16\cos3.08} = 0.8685$$

Table B-1 Crystallite size of standard zeolite NaY, zeolite NaY, and Meso-NaY

Adsorbent	Crystallite size (nm)
Standard zeolite NaY	1.1547
Zeolite NaY	0.7720
Meso-NaY (Leaching)	0.8685
Meso-NaY (CTAB)	1.1540
Meso-NaY (PDADMAC)	1.5440

BIOGRAPHY

Name: Miss Tharaporn Yangyaim

Date of Birth: January 14, 1987

Nationality: Thai

Education: 2005-2008, Bachelor Degree of Environmental Science, Faculty of Environment and Resource Studies, Mahidol University

Conference: The 17th Regional Symposium on Chemical Engineering (RSCE 2010)